Journal of Inorganic Biochemistry 230 (2022) 111743

Contents lists available at ScienceDirect

Journal of Inorganic Biochemistry

journal homepage: www.elsevier.com/locate/jinorgbio

Selective detection of *Aeromonas* spp. by a fluorescent probe based on the siderophore amonabactin

Javier Cisneros-Sureda [a], Diego Rey-Varela [b], Jaime Rodríguez [a,*], Miguel Balado [b], Manuel L. Lemos [b,*], Carlos Jiménez [a,*]

[a] Centro de Investigacións Científicas Avanzadas (CICA), Departamento de Química, Facultade de Ciencias, Universidade da Coruña, 15071 A Coruña, Spain
[b] Departamento de Microbiología y Parasitología, Instituto de Acuicultura, Universidade de Santiago de Compostela, 15782 Santiago de Compostela, Spain

ARTICLE INFO

Keywords:
Iron
Siderophores
Amonabactin
Aeromonas
Fluorescent probe
Bacteria detection

ABSTRACT

Amonabactins, the siderophores produced by some pathogenic bacteria belonging to *Aeromonas* genus, can be used for the preparation of conjugates to be imported into the cell using their specific transport machinery. Herein, we report the design and synthesis of a new amonabactin-based fluorescent probe by conjugation of the appropriate amonabactin analogue to sulforhodamine B (AMB-SRB) using a thiol-maleimide click reaction. Growth promotion assays and fluorescence microscopy studies demonstrated that the AMB-SRB fluorescent probe was able to label the fish pathogenic bacterium *A. salmonicida* subsp. *salmonicida* through its outer membrane transport (OMT) protein FstC. The labelling of other *Aeromonas* species, such as the human pathogen *A. hydrophila*, indicates that this probe can be a very useful molecular tool for studying the amonabactin-dependent iron uptake mechanism. Furthermore, the selective labelling of *A. salmonicida* and other *Aeromonas* species in presence of other fish pathogenic bacteria, suggest the potential application of this probe for detection of *Aeromonas* in water and other fish farming samples through fluorescence assays.

1. Introduction

Gram-negative bacteria belonging to the genus *Aeromonas* are widely distributed in aquatic environments and some species are responsible for diseases not only in fish and other aquatic organisms but also in humans.[1] They have been isolated from fruits, vegetables, meats and other food products,[2] with high incidence in wastewaters.[3] A wide range of human diseases, usually related with gastroenteritis, septicemia, and wound infections are caused by these emerging pathogens. Among *Aeromonas* species, *Aeromonas caviae, A. dhakensis, Aeromonas veronii* and *A. hydrophila* are the four most prevalent species since they have been identified as 94.7% of the isolates associated to clinical cases.[4] Although the worldwide incidence of human infections caused by *Aeromonas* is unknown, an estimated incidence of 10.5 cases per million people was reported in England in 2004 and 1.5 cases per million people in France in 2006.[5].

Aquaculture is becoming an important food source worldwide. Its global production rose more than five times in the last three decades providing now more than 50% of fish for human consumption, whereas fishing captures were stabilized in the last 20 years.[6] However, the occurrence of emerging infectious disease outbreaks and the appearance of antimicrobial resistances (AMR) in bacterial pathogens are two of the most important drawbacks for aquaculture development. Indeed, the search for new strategies to detect, prevent and control diseases in aquatic species is urgently needed.[7] More specifically, *Aeromonas salmonicida* subsp. *salmonicida* (*A. salmonicida*) is responsible for furunculosis, a disease which causes economically devastating losses in cultivated salmonids and other fish species in fresh and marine waters.[8] Early, specific and sensitive diagnostic methods are essential for the rapid treatment of this bacterial pathogen.

Iron is an essential micronutrient required for the growth of almost all aerobic organisms. However, its bioavailability is very low and bacteria developed several uptake mechanisms to obtain iron. Among them, one of the most extended is based on the synthesis of siderophores, small molecules capable of stealing iron from the high-affinity iron(III)-binding proteins of the host.[9] In Gram-negative bacteria, ferri-siderophore complexes must be internalized through specific TonB-dependent outer membrane transporters (OMT). All these transporters show a typical plugged β-barrel structure,[10] and are coupled to an ABC (ATP-binding-cassette) system that catalyzes the transport through

* Corresponding authors.
E-mail address: carlos.jimenez@udc.es (C. Jiménez).

https://doi.org/10.1016/j.jinorgbio.2022.111743
Received 12 November 2021; Received in revised form 18 January 2022; Accepted 21 January 2022
Available online 29 January 2022

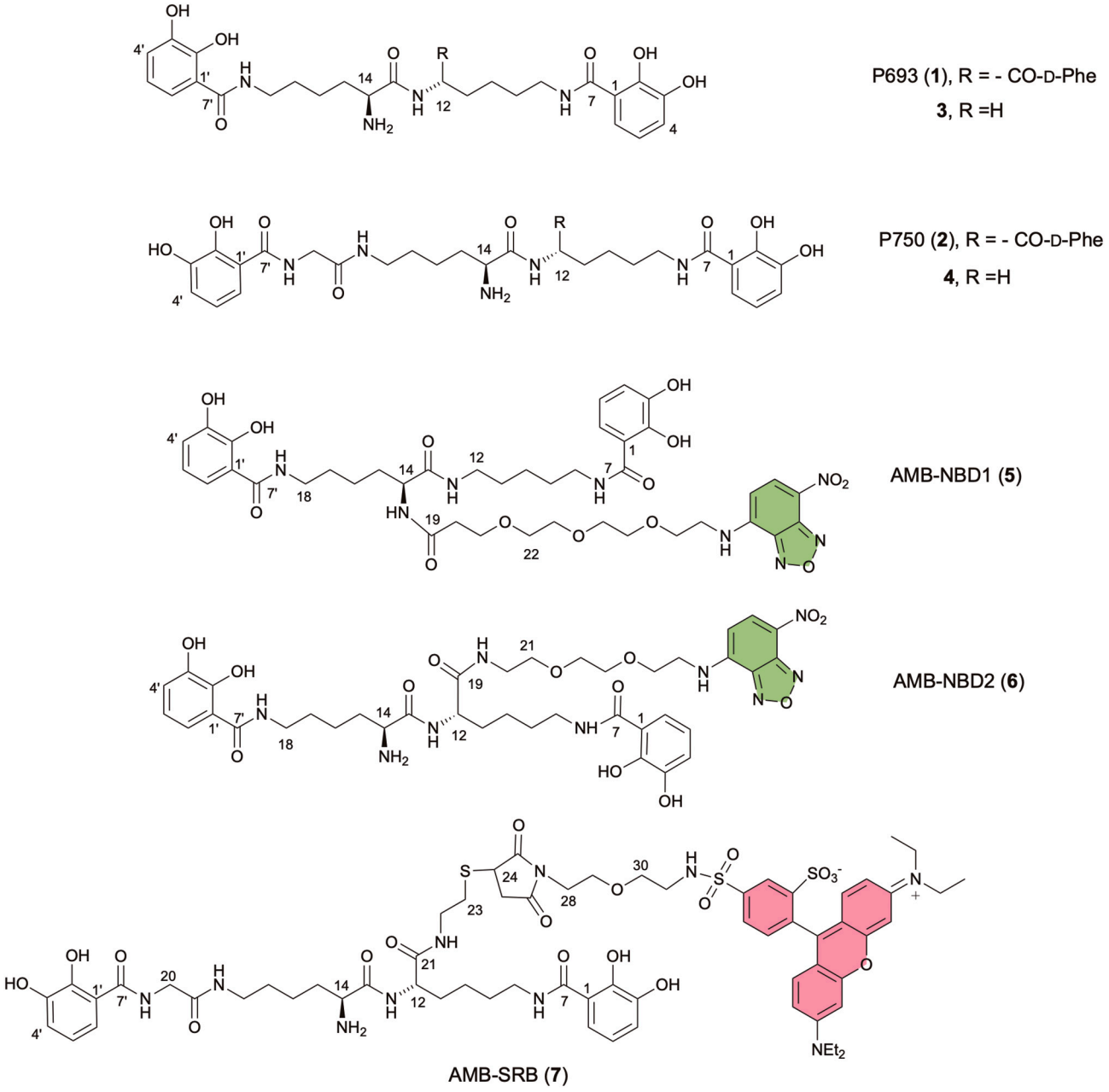

Fig. 1. Structure of two natural amonabactins P683 (**1**) and P750 (**2**), two synthetic analogues (**3** and **4**) and their derivative conjugates (**5**–**7**) prepared in this work.

the plasma membrane. These mechanisms are becoming interesting Achilles heels of bacteria, since they can be used for the rational design of antimicrobial conjugates against pathogenic bacteria. One of the most promising approaches is the use of siderophore-drug conjugates (SDCs) known as the Trojan horse strategy[11], since they use the transport machinery of siderophores to introduce antibacterial compounds into the cell. The FDA-approved cephalosporin antibiotic cefiderocol is the most successful catechol-based SDC so far.[12].

Four peptide-based biscatecholate, named amonabactins (AMBs) were the first siderophores characterized from species of *Aeromonas*, more specifically from *A. hydrophila*, being amonabactin P693 (**1**) and P750 (**2**) the most representative forms (Fig. 1).[13] Later on, we identified AMBs, along with acinetobactin, as the siderophores responsible for the iron uptake in *A. salmonicida.*[14] We were also able to deduce their biosynthetic routes and identify their corresponding OMTs, FstC for AMBs [15], and FstB for acinetobactin.[16] These transporters specifically bind and transport to the bacterial periplasm the cognate ferri-siderophores. The synthesis of several analogues of AMBs allowed us to deduce several structure-activity relationships (SARs) and to find that OMT FstC could be exploited for delivery of antimicrobial compounds into the cell. Moreover, these studies allowed us to select two simplified AMB derivatives (**3** and **4**) that could serve as vectors to deliver different compounds into the bacterial cells (Fig. 1). The presence of the amino group in **3** and **4** as a functional group amenable for synthetic modification could be used for cargos attachment in order to prepare conjugates to study the iron uptake mechanism or other applications in different pathogens of the genus *Aeromonas*, including the human pathogen *A. hydrophila.*[15].

In the present work, we designed the synthesis of different fluorescent-conjugated AMB analogues, **5**–**7**, which were tested in growth promotion assays and epifluorescence microscopy studies with *A. salmonicida* (Fig. 1). The work aimed to find a fluorescent probe that could be selectively internalized not only by *A. salmonicida* via amonabactin OMT FstC, but also by other pathogenic *Aeromonas* spp. Although

siderophore analogues were previously employed in the preparation of fluorescent probes,[17],[18],[19],[20],[21] this is the first time that they are designed to target bacteria of the genus *Aeromonas*.

2. Experimental section

2.1. Biology methods

2.1.1. Bacterial strains, plasmids, and media

The strains used in this work are summarized in Table S1. All bacteria were routinely grown at 25 °C in Tryptic Soy Agar (TSA) or Tryptic Soy Broth (TSB) (Pronadisa) supplemented with NaCl (Thermo) up to 1% (TSA-1 or TSB-1). For assays under iron-limiting conditions, the strains were cultured in M9 minimal medium[22] supplemented with 0.2% Casamino Acids (Difco) resulting into CM9 medium. Iron restriction was induced in the CM9 medium by the addition of ethylenediamine-di(*o*-hydroxyphenylacetic acid) (EDDHA) (Sigma-Aldrich) at the suitable concentration. EDDHA stock solution was prepared dissolving 1 g in 15 mL of NaOH 1 N and adjusting the pH to 9.0 with HCl 37% in a final volume of 20 mL.

2.1.2. Growth under Iron-limiting conditions

The characterization of biological activity of amonabactins, analogues and probes were carried out in CM9 with the addition of EDDHA 5 μM. The EDDHA minimal inhibitory concentration (MIC) was determined by growing the strains in a gradient of EDDHA (0.5 to 10 μM). Strains VT45.1*ΔentB,* which carries the amonabactin receptor (FstC) active, and VT45.1*ΔentBΔfstC,* with FstC inactivated, were cultured in TSB-1 at 25 °C with shaking until an OD_{600} of 0.5 (mid log phase) and inoculated in a proportion 1:40 into wells of 96-well microtiter plates, containing 200 μL of medium per well. Siderophores, analogues or probes were included into the pertinent well at the appropriate concentration (13.0, 6.5, 3.25 or 1.62 μM). The compound stocks were prepared in a methanol:milliQ-water (1:1) solution at 1.3 mM and stored at −20 °C. Microplates were incubated for 18 h at 25 °C into an iMACK Microplate reader (Bio-Rad) taking measurements every 30 min. All the conditions were assayed in triplicate in each experiment and three independent experiments were performed. All assays incorporated the suitable control wells: media without the addition of siderophore/analogue/probe, media supplemented with $FeCl_3$ 10 μM and media without bacteria. Student's test was performed to analyze the statistical differences between the different conditions.

2.1.3. Fluorescence assays

Sample preparation for fluorescence microscopy was performed in CM9 medium under weak iron restriction (EDDHA 1 μM). The strains tested in this work are listed in Table S1. The bacteria were cultured with shaking in TSB-1 at 25 °C until an OD_{600} of 0.5 (mid log phase) and inoculated into 5 mL of CM9 in a proportion 1:40. After adding the probes at a concentration of 6.5 μM, the bacteria were incubated for 12 h at 25 °C with shaking at 150 rpm. When the cultures reached an OD_{600} of approximately 0.85, 1 mL was centrifuged for 3 min at 8000 rpm and the cells were washed by resuspension in cold (4 °C) Phosphate-Buffered Saline (PBS). This washing procedure was repeated three times to eliminate any residual non-attached probe. After centrifugation, the cells were fixed for 15 min in 1 mL of PBS with 2% *p*-formaldehyde (Sigma-Aldrich) at 4 °C. Finally, the cells were washed twice and visualized at the fluorescence microscope. Imaging was performed on a Confocal Microscope A1R (Nikon) using a 1000× oil immersion objective lens. The filter set used was the G2A (Ex. 560 nm, Em. 575–615 nm).

2.2. Chemistry methods

2.2.1. General information and procedures

Nuclear Magnetic Resonance (NMR) spectra (proton and carbon) were recorded on Bruker Advance I 500, Advance III HD 400, and Advance Neo 300 spectrometers at the University of A Coruña, using $CDCl_3$ and CD_3OD as the solvents and internal standards. Multiplicities of ^{13}C signals were obtained by DEPT-135. Medium-pressure chromatographic separations were carried out on silica gel 60 (230–400 mesh). Low Resolution Electrospray Ionization Mass Spectrometry (LRESIMS) and High Resolution Electrospray Ionization Mass Spectrometry (HRESIMS) were measured on Applied Biosystems QSTAR Elite and LTQ Orbitrap Discovery. High Performance Liquid Chromatography (HPLC) separations were carried out on an Agilent HP1100 liquid chromatography system equipped with a solvent degasser, quaternary pump, and an UV detector (Agilent Technologies, Waldbronn, Germany). In the HPLC separations, a Discovery® column HS F5 (100 × 4.6 mm, 5 μm) was used.

All moisture-sensitive reactions were carried out under an atmosphere of argon in flame-dried glassware closed by rubber septum, unless otherwise noted. Solvents were distilled prior to use under argon atmosphere and dried according to standard procedures. Solutions and solvents were added via syringe or cannula. Thin Layer Chromatography (TLC) was performed using silica gel GF-254 Merck, spots were revealed employing UV light (254 nm) and/or by heating the plate pre-treated with an ethanolic solution of phosphomolybdic acid, a solution of cerium sulphate or a solution of ninhydrin in BuOH-AcOH-H_2O. CRYOCOOL apparatus was used for low-temperature reactions.

2.2.2. Organic synthesis

Synthesis of intermediates **8**, **9** and **22** are described in previous work (see ref. [15]).

Synthesis of amonabactin analogue 3- nitrobenzofurazan conjugate 1 (AMB-NBD1) (5).

Synthesis of 10: A solution of **9** (50 mg, 0.064 mmol) in 5 mL of a mixture of trifluoroacetic acid (TFA)/CH_2Cl_2 (1:9) was stirred at room temperature for 90 min. Then, the mixture was concentrated under reduced pressure to obtain **10** (42 mg, 0.063 mmol, quant.) as a white solid. It was used in next step without characterization.

Synthesis of 11: To a solution of 4-chloro-7-nitrobenzofurazan (200 mg, 1.00 mmol) and cesium carbonate (386 mg, 2.00 mmol) in anhydrous CH_3CN (5 mL), was added a solution of *tert*-butyl 12-amino-4,7,10-trioxadodecanoate (278 mg, 1.00 mmol) in anhydrous CH_3CN (5 mL), and the mixture was stirred overnight at room temperature. Then, the reaction was concentrated under reduced pressure, and the residue was purified by silica gel column chromatography eluting with MeOH/CH_2Cl_2 (4:96) to give **11** (315 mg, 0.72 mmol, 72% yield), as a yellow oil. ^1H NMR (300 MHz, $CDCl_3$): δ 8.46 (d, J = 8.7 Hz, 1H, H-5); 7.21 (s, 1H, NH); 6.18 (d, J = 8.7 Hz, 1H, H-6); 3.87 (t, J = 4.6 Hz, 2H, H-13); 3.72–3.61 (m, 12H, H-7-12); 2.48 (t, J = 6.5 Hz, 2H, H-14); 1.42 (s, 9H, ^{t}Bu). ^{13}C NMR (75 MHz, $CDCl_3$): δ 171.1 (CO, C-15); 144.4 (C, C-3/C-2); 144.1 (C, C-1); 136.6 (CH, C-5); 123.8 (C, C-4); 98.9 (CH, C-6); 80.7 (C, ^{t}Bu); 70.8–70.5 (CH_2, C-9-12); 68.3 (CH_2, C-8); 67.0 (CH_2, C-13); 44.0 (CH_2, C-7); 36.4 (CH_2, C-14); 28.2 (CH_3, ^{t}Bu). HRMS (ESI$^+$) m/z: $[M + Na]^+$ calcd. For $C_{19}H_{28}N_4O_8Na$: 463.1799; found: 463.1800.

Synthesis of 12: A solution of **11** (100 mg, 0.21 mmol) in TFA/CH_2Cl_2 (1:9, 5 mL) was stirred for 90 min. After the reaction was completed as monitored by TLC, the mixture was concentrated under reduced pressure to obtain a yellow oil. Then, *N*-hydroxysuccinimide (NHS) (47 mg, 0.42 mmol) and 1-ethyl-3-(3-dimethylaminopropyl) carbodiimide hydrochloride (EDC·HCl) (60 mg, 0.31 mmol) were added, dissolved in anhydrous CH_2Cl_2 (6 mL), and the mixture was stirred at room temperature overnight. The reaction was washed with water and brine, dried with $MgSO_4$, filtered, and concentrated under reduced pressure. The residue was purified by silica gel column chromatography eluting with MeOH/CH_2Cl_2 (5:95) to give **12** (80 mg, 0.17, 80%) as a yellow oil. ^1H NMR (400 MHz, $CDCl_3$): δ 8.45 (d, J = 8.7 Hz, 1H, H-5); 7.43 (s, 1H, NH); 6.19 (d, J = 8.7 Hz, 1H, H-6); 3.87 (t, J = 4.6 Hz, 2H, H-13); 3.76–3.58 (m, 12H, H-8-12); 2.74 (s, 4H, NHS); 2.60 (t, J = 6.5 Hz, 2H, H-14). ^{13}C NMR (100 MHz, $CDCl_3$): δ 175.3 (—CO, C-15); 172.5 (—CO, NHS); 144.5–144.0 (C, C-1-3); 136.7 (CH, C-5); 123.3 (C,

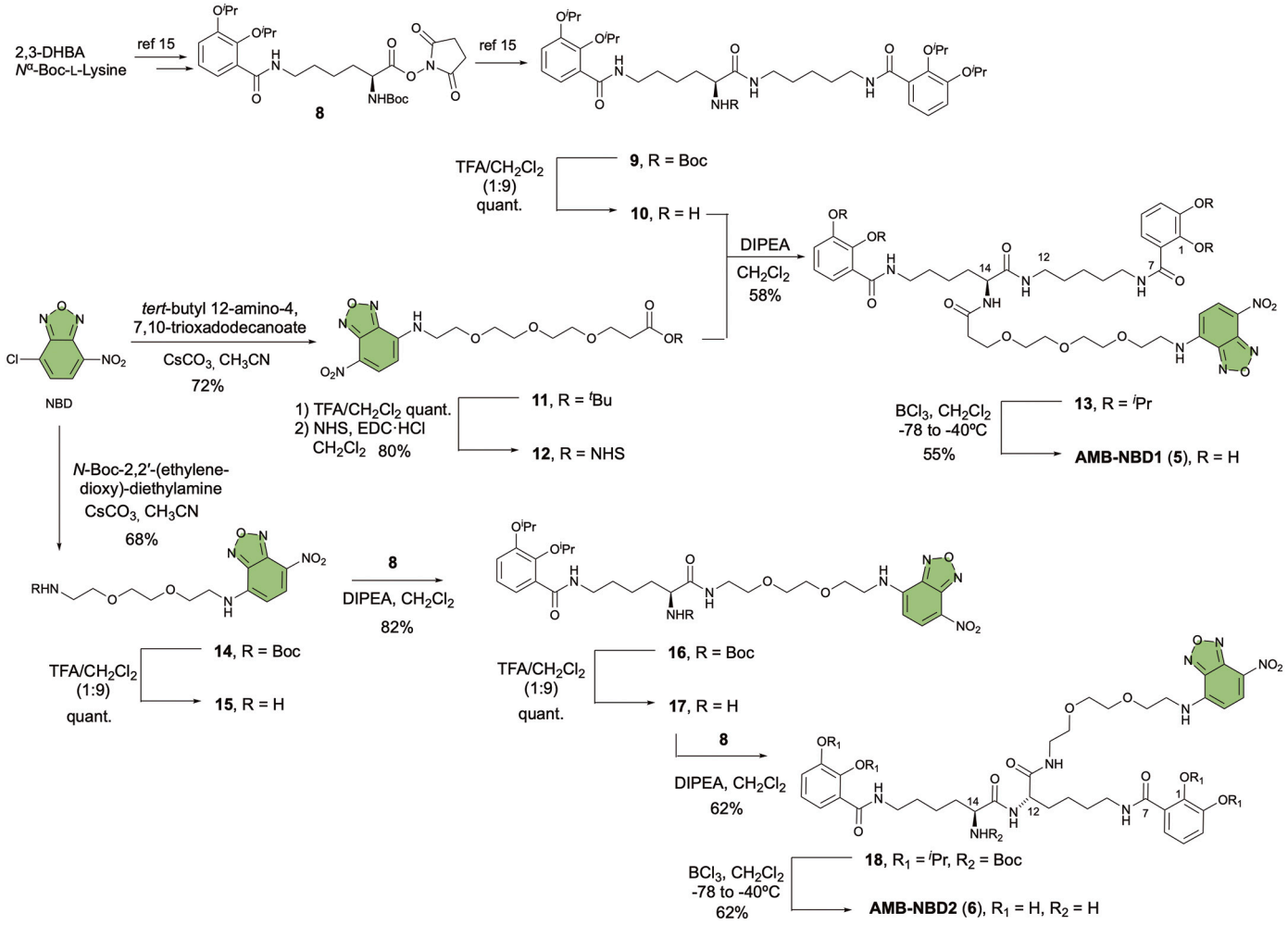

Scheme 1. Synthesis of **AMB-NBD1** (**5**) and **AMB-NBD2** (**6**)

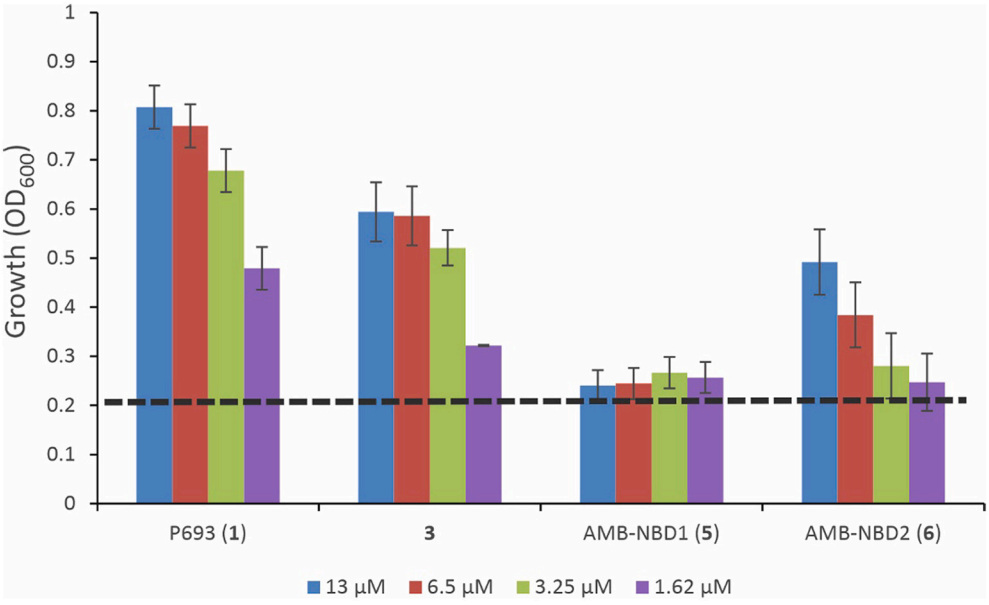

Fig. 2. Bacterial growth promotion of natural amonabactin AMB P-693 (**1**), amonabactin analogue **3** and conjugates **AMB-NBD1** (**5**) and **AMB-NBD2** (**6**) as iron sources for *A. salmonicida* carrying a functional FstC transporter (VT45.1Δ*entB*). Depicted growth values were achieved by *A. salmonicida* VT45.1Δ*entB*Δ*fstB* after 12 h of incubation under iron starvation (CM9 with EDDHA 5 µM) supplemented with 1.62 (purple), 3.25 (green), 6.5 (red) or 13.0 µM (blue) of the assayed compound. Dotted line represents basal growth without adding any compound. All experiments were performed in triplicate. Standard deviations are shown for each bar. (For interpretation of the references to colour in this figure legend, the reader is referred to the web version of this article.)

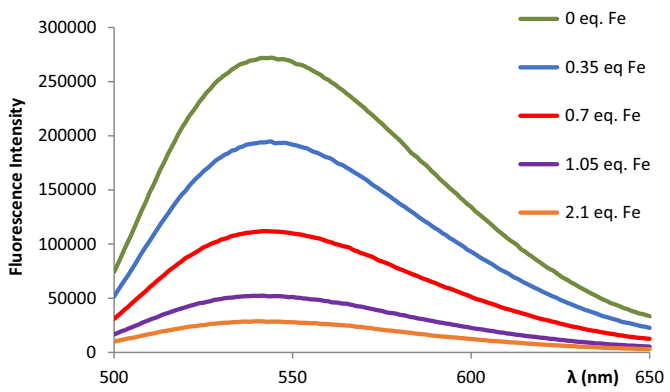

Fig. 3. Fluorescence iron (III) titration curves with **AMB-NBD2** (**6**). Aliquots of stock solutions of **6** in MeOH were treated with aliquots of methanolic solutions of $FeCl_3$ (0, 0.35, 0.7, 1.05, and 2.1 equiv.) and diluted with MeOH to a final ligand concentration of 20 μM.

C-4); 98.9 (CH, C-6); 70.6–70.2 (CH_2, C-9-12); 68.2 (CH_2, C-8); 66.3 (CH_2, C-13); 43.9 (CH_2, C-7); 34.6 (CH_2, C-14); 25.4 (CH_2, NHS). HRMS (ESI^+) *m/z*: $[M + H]^+$ calcd. For $C_{19}H_{24}N_5O_{10}$: 482.1517; found: 482.1521.

Synthesis of 13: To a solution of **12** (50 mg, 0.074 mmol) in CH_2Cl_2 (5 mL), was added a solution of **10** (42 mg, 0.082 mmol) in CH_2Cl_2 (5 mL) and *N*,*N*-diisopropylethylamine (DIPEA) (27 μL, 0.150 mmol), and the mixture was stirred at room temperature for 4 h. Then, it was concentrated under reduced pressure and the residue was purified by silica gel column chromatography eluting with MeOH/CH_2Cl_2 (5%), to obtain **13** (45 mg, 0.043 mmol, 58%) as a yellow oil. ^1H NMR (400 MHz, $CDCl_3$): δ 8.41 (d, $J = 8.7$ Hz, 1H, H-33); 8.06 (brt, 1H, NH); 8.01 (brt, 1H, NH); 7.59 (2 x dd, $J = 8.0$, 1.5 Hz, 2H, H-6/6′); 7.14 (d, $J = 7.3$ Hz, 1H, NH); 7.09–6.90 (m, 5H, H-4/H-5/NH); 6.79 (t, $J = 5.7$ Hz, 1H, NH); 6.17 (d, $J = 8.7$ Hz, 1H, H-32); 4.64 (2 x hept, $J = 6.2$ Hz, 2H, ^{i}Pr); 4.52 (2 x hept, $J = 6.2$ Hz, 2H, ^{i}Pr); 4.32 (m, 1H, H-14); 3.83–3.57 (m, 12H, H-22-27); 3.47–3.29 (m, 4H, H-8/H-18); 3.20 (m, 2H, H-12); 2.51–2.40 (m, 2H, H-20); 1.95–1.82 (m, 2H, H-11); 1.75–1.36 (m, 10H, H-9/H-10/H-15/H-16/H-17); 1.33 (d, $J = 6.2$ Hz, 12H, ^{i}Pr); 1.26 (d, $J = 6.2$ Hz, 12H, ^{i}Pr). ^{13}C NMR (100 MHz, $CDCl_3$): δ 171.8 (2CO, C-13/C-19); 166.1 (2CO, C-7/C-7′); 150.8 (2C, C-2/2′); 146.0 (2C, C-3/3′); 144.3 (C, C-28-31); 136.6 (CH, C-33); 128.3 (2C, C-1/1′); 123.7 (2CH, C-4); 123.7 (C, C-32); 122.7 (2CH, C-5/5′); 118.3 (2CH, C-6/6′); 98.6 (CH, C-32); 76.4 (2CH, ^{i}Pr); 71.2 (2CH, ^{i}Pr); 70.6–70.3 (CH_2, C-23-26); 68.4/67.4 ($2CH_2$, C-21/22); 53.4 (CH, C-14); 44.0 (CH_2, C-27); 39.5/39.3 ($2CH_2$, C-18/C-8); 38.9 (CH_2, C-12); 31.3/29.8/29.5/24.3/22.9 ($5CH_2$, C-9/10/11/15/16/17); 22.5 (CH_3, ^{i}Pr); 22.2 (CH_3, ^{i}Pr). HRMS (ESI^+) *m/z*: $[M + H]^+$ calcd. For $C_{52}H_{77}N_8O_{14}$: 1037.5553; found: 1037.5559. $[\alpha]_D^{25} = +34.5$ ($c = 0.14$, $CHCl_3$).

Synthesis of AMB-NBD1 (5): To a solution of **13** (35 mg, 0.034

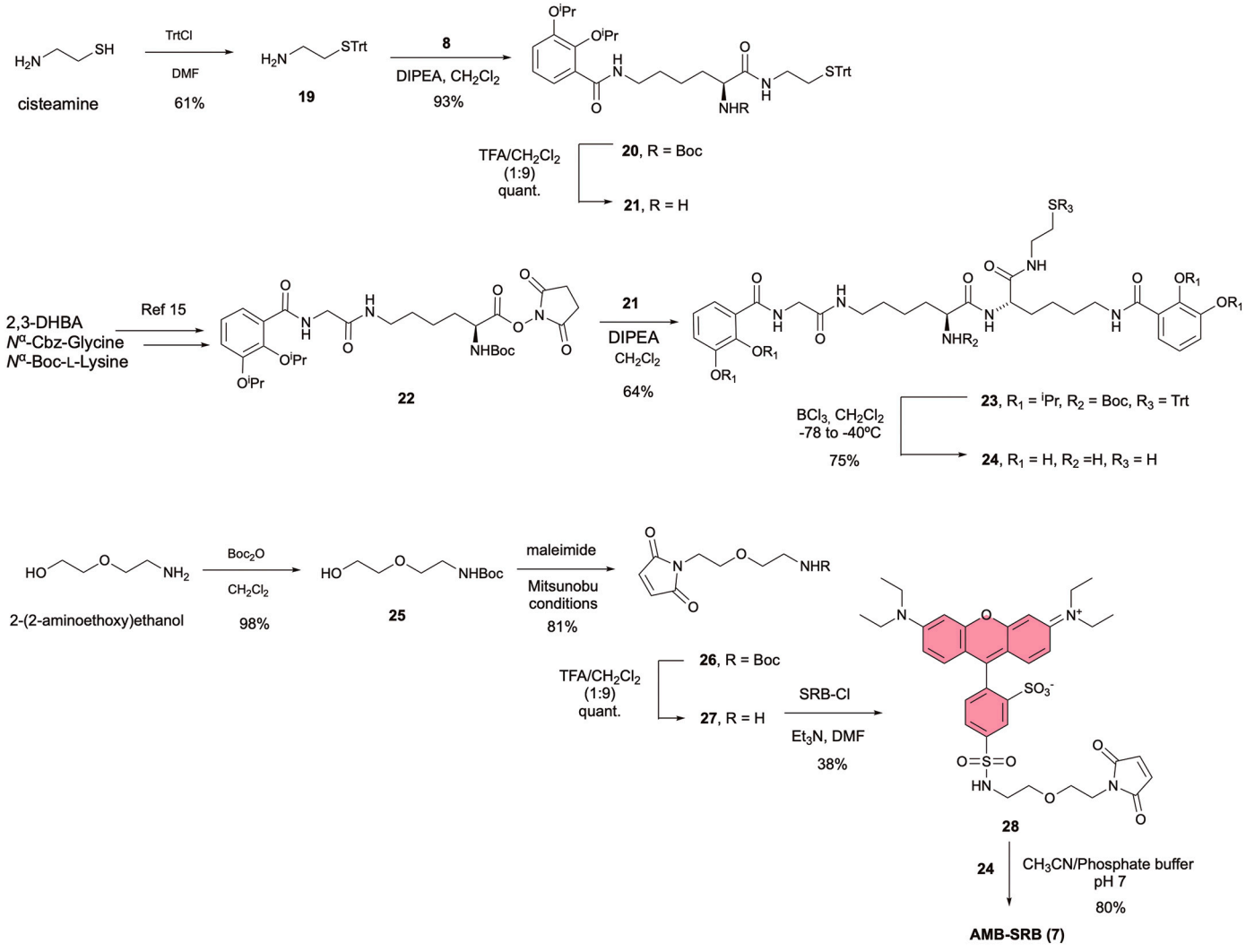

Scheme 2. Synthesis of **AMB-SRB** (**7**).

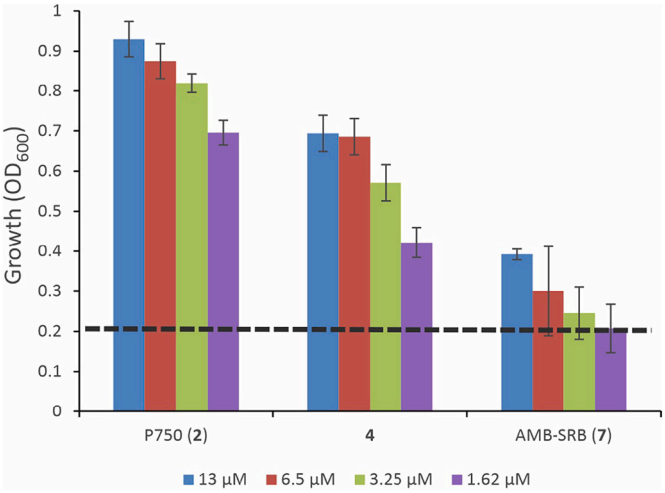

Fig. 4. Bacterial growth promotion assay of natural AMB P-750 (**2**), amonabactin analogue **4** and **AMB-SRB** (**7**) as iron sources for *A. salmonicida* VT45.1Δ*entB* carrying a functional FstC, the amonabactin OMT. Depicted growth values were achieved after 12 h of incubation under iron starvation (CM9 with EDDHA 5 μM) supplemented with 1.62 (light purple), 3.25 (green), 6.5 (red) or 13.0 μM (blue) of the assayed compound. Dotted line represents basal growth without adding any compound. All experiments were performed in triplicate. Standard deviations are shown for each bar. (For interpretation of the references to colour in this figure legend, the reader is referred to the web version of this article.)

mmol) in anhydrous CH_2Cl_2 (5 mL) at −78 °C, was added BCl_3 (340 μL, 1 M in CH_2Cl_2), and the mixture was stirred overnight at −40 °C. Then, 5 mL of water was added to quench the reaction and concentrated under reduced pressure. The residue was purified by HPLC using a Discovery HS F5 (100 × 4.6 mm, 5 μm) column with a mobile phase consisting on a gradient of 50% CH_3CN to 100% in H_2O (*v*/v), each containing 0.1% TFA, for 15 min, at a flow rate of 2 mL/min (injected volume 1 mL; detection 254 nm, retention time 9 min), to give **5** (16 mg, 0.018 mmol, 55%) as an orange oil. ^{1}H NMR (400 MHz, CD_3OD): δ 8.47 (d, J = 8.7 Hz, 1H, H-33); 7.20 (2 x dd, J = 8.0, 1.5 Hz, 2H, H-6/6′); 6.91 (2 x dd, J = 8.0, 1.5 Hz, 2H, H-4/4′); 6.70 (2 x t, J = 8.0 Hz, 2H, H-5); 6.37 (d, 1H, J = 8.7 Hz, H-34); 4.30 (dd, J = 8.7, 5.3 Hz, 1H, H-14); 3.83 (t, J = 5.7 Hz, 2H, H-22); 3.80–3.50 (m, 14H, H-23-27); 3.40–3.34-3.20 (m, 4H, H-8/H-18/H-12); 2.47 (t, J = 5.7 Hz, 2H, H-20); 1.90–1.77 (m, 2H, H-11); 1.72–1.49 (m, 6H, H-9/H-15/H-17); 1.48–1.33 (m, 4H, H-10/H-16). ^{13}C NMR (100 MHz, CD_3OD): δ 172.8 (CO, C-19); 172.6 (CO, C-13); 170.0 (2CO, C-7/C-7′); 148.8 (2C, C-2/2′); 145.9 (2C, C-3/3′); 144.2 (C, C-28-31); 137.0 (CH, C-32); 121.8 (2C, C-1/1′); 118.1 (4CH, C-4/4′, C-5/5′); 117.2 (C, C-32); 115.3 (2CH, C-6/6′); 98.8 (CH, C-33); 70.2–69.9 (CH_2, C-22-25); 68.4 (CH_2, C-26); 66.8 (CH_2, C-21); 53.4 (CH, C-14); 43.4 (CH_2, C-27); 38.9–38.7 ($3CH_2$, C-8/C-12/C-18); 36.1 (CH_2, C-12); 31.5–28.6 ($3CH_2$, C-9/C-11/C-15/C-17/C-20); 23.8/22.8 ($2CH_2$, C-16/C-10). HRMS (ESI$^+$) *m/z*: $[M + Na]^+$ calcd. For $C_{390}H_{53}N_8O_{14}Na$: 891.3495; found: 891.3506. $[\alpha]_D^{25}$ = +29.1 (c = 0.11, CH_3OH).

Synthesis of amonabactin analogue 3- nitrobenzofurazan conjugate 2 (AMB-NBD2 (6).

Synthesis of 14: To a solution of 4-chloro-7-nitrobenzofurazan (40 mg, 0.20 mmol) and cesium carbonate (130 mg, 0.40 mmol) in anhydrous CH_3CN (5 mL), was added a solution of *tert*-butyl 12-amino-4,7,10-trioxadodecanoate (50 mg, 0.20 mmol) in anhydrous CH_3CN (5 mL), and the mixture was stirred overnight at room temperature. Then, the reaction was concentrated under reduced pressure, and the residue was purified by silica gel column chromatography eluting with EtOAc/Hex (80%) to give **14** (56 mg, 0.14 mmol, 68%), as a yellow oil. ^{1}H NMR (300 MHz, $CDCl_3$): δ 8.42 (d, J = 8.7 Hz, 1H, H-5); 7,13 (brs, 1H, NH); 6.18 (d, J = 8.7 Hz, 1H, H-6); 5.05 (brs, 1H, NH-*tert*-butyloxycarbonyl (Boc)); 3.85/ 3.74/3.61 (m, 8H, H-8/H-9/H-10/H-11); 3.56 (t, J = 5.6 Hz, 2H, H-7); 3.38–3.25 (m, 2H, H-12); 1.39 (s, 9H, Boc). ^{13}C NMR (75 MHz, $CDCl_3$): δ 156.1 (CO, Boc); 144.2 (C, C-3/C-2); 143.9 (C, C-1); 136.5 (CH, C-5); 123.6 (C, C-4); 98.9 (CH, C-6); 79.3 (C, Boc); 70.5–70.2 (CH_2, C-9-11); 68.2 (CH_2, C-8); 43.7 (CH_2, C-7); 40.3 (CH_2, C-12); 28.4 (CH_3, Boc). HRMS (FAB$^+$) *m/z*: $[M + H]^+$ calcd. For $C_{17}H_{26}N_5O_7$: 412.1827; found: 412.1852.

Synthesis of 15: A solution of **14** (50 mg, 0.12 mmol) in TFA: CH_2Cl_2 (1:9, 5 mL) was stirred for 90 min. After the reaction was complete as monitored by TLC, the mixture was concentrated under reduced pressure to obtain **15** (36 mg, quant.) as a yellow oil. It was used in next step without purification.

Synthesis of 16: To a solution of **8** (70 mg, 0.12 mmol) in CH_2Cl_2 (5 mL), was added a solution of **15** (36 mg, 0.11 mmol) in CH_2Cl_2 (5 mL) and DIPEA (35 μL, 0.200 mmol), and the mixture was stirred at room temperature for 4 h. Then, it was concentrated under reduced pressure, and the residue was purified by silica gel column chromatography eluting with MeOH/CH_2Cl_2 (5%), to obtain **16** (72 mg, 0.095 mmol, 82%) as a yellow oil. ^{1}H NMR (300 MHz, $CDCl_3$): δ 8.41 (d, J = 8.7 Hz, 1H, H-24); 8.14 (t, J = 5.3 Hz, 1H, NH); 7.62 (dd, J = 8.0, 1.5 Hz, 1H, H-6); 7.50 (s, 1H, NH); 7.04–6.96 (m, 2H, H-5/H-4); 6.74 (brt, 1H, NH); 6.18 (d, J = 8.7 Hz, 1H, H-25); 5.44 (d, J = 7.7 Hz, 1H, NH-Boc); 4.65 (hept, J = 6.2 Hz, 1H, ^{i}Pr); 4.53 (hept, J = 6.2 Hz, 1H, ^{i}Pr); 4.04 (m, 1H, H-12); 3.90–3.79 (m, 2H, H-15); 3.75–3.30 (m, 12H, H-14/H-16-19); 1.95–1.55 (m, 6H, H-9-11); 1.40 (s, 9H, Boc); 1.34 (d, J = 6.2 Hz, 6H, ^{i}Pr); 1.27 (d, J = 6.2 Hz, 6H, ^{i}Pr). ^{13}C NMR (75 MHz, $CDCl_3$): δ 172.4 (CO, C-13); 166.2 (CO, C-7); 155.8 (CO, Boc); 150.7 (C, C-2); 146.0 (C, C-2); 144.4 (C, C-20-22); 136.6 (CH, C-24); 128.1 (C, C-1); 123.6 (CH, C-4); 123.1 (C, C-23); 122.6 (CH, C-5); 118.2 (CH, C-6); 98.7 (CH, C-25); 79.7 (C, Boc); 76.3 (CH, ^{i}Pr); 71.1 (CH, ^{i}Pr); 70.5–70.3 (CH_2, C-16-17); 69.7 (CH_2, C-18); 68.3 (CH_2, C-15); 54.6 (CH, C-12); 43.8 (CH_2, C-19); 39.1 (CH_2, C-8); 38.7 (CH_2, C-14); 31.8 (CH_2, C-11); 29.4 (CH_2, C-9); 28.3 (CH_3, Boc); 22.7 (CH_2, C-10); 22.3 (CH_3, ^{i}Pr); 22.0 (CH_3, ^{i}Pr). HRMS (FAB$^+$) *m/z*: $[M + H]^+$ calcd. For $C_{36}H_{54}N_7O_{11}$: 760.3876; found: 760.3860. $[\alpha]_D^{25}$ = +35.0 (c = 0.14, $CHCl_3$).

Synthesis of 17: A solution of **16** (70 mg, 0.092 mmol) in TFA: CH_2Cl_2 (1:9, 5 mL) was stirred for 90 min. After the reaction was completed as monitored by TLC, the mixture was concentrated under reduced pressure to obtain **17** (60 mg, 0.091 mmol, quant.) as a yellow oil. It was used in next step without purification.

Synthesis of 18: To a solution of **8** (55 mg, 0.097 mmol) in CH_2Cl_2 (5 mL), was added a solution of **17** (60 mg, 0.091 mmol) in CH_2Cl_2 (5 mL) and DIPEA (35 μL, 0.200 mmol), and the mixture was stirred at room temperature for 4 h. Then, it was concentrated under reduced pressure, and the residue was purified by silica gel column chromatography eluting with MeOH/CH_2Cl_2 (5%), to obtain **18** (62 mg, 0.056 mmol, 62%) as a yellow oil. ^{1}H NMR (300 MHz, $CDCl_3$): δ 8.45 (d, J = 8.7 Hz, 1H, H-30); 8.13 (t, J = 5.3 Hz, 2H, NH); 7.65 (dd, J = 8.1, 1.5 Hz, 2H, H-6/6′); 7.11–6.92 (m, 6H, H-5/5'/H-4/4'/NH/19); 7.11–6.92 (m, 2H, H-31/NH-Boc); 4.65 (2 x hept, J = 6.2 Hz, 2H, ^{i}Pr); 4.54 (2 x hept, J = 6.2 Hz, 2H, ^{i}Pr); 4.36 (m, 1H, H-14); 4.01 (m, 1H, H-12); 3.91–3.82 (m, 2H, H-21); 3.75–3.50 (m, 8H, H-22-25); 3.45–3.20 (m, 6H, H-8/H-18/H-20); 2.05–1.50 (m, 12H, H-9-11/H-15/H-17); 1.44 (s, 9H, Boc); 1.34 (d, J = 6.2 Hz, 12H, ^{i}Pr); 1.27 (d, J = 6.2 Hz, 12H, ^{i}Pr). ^{13}C NMR (75 MHz, $CDCl_3$): δ 173.2 (CO, C-19); 171.7 (CO, C-13); 166.3 (2CO, C-7/7′); 156.5 (CO, Boc); 150.9 (2C, C-2/2′); 146.0 (2C, C-3/3′); 144.3 (C, C-26-28); 136.7 (CH, C-30); 128.2 (2C, C-1/1′); 123.7 (2CH, C-4/4′); 122.6 (2CH, C-5/5′); 122.3 (C, C-29); 118.2 (2CH, C-6/6′); 98.7 (CH, C-31); 80.2 (C, Boc); 76.4 (2CH, ^{i}Pr); 71.1 (2CH, ^{i}Pr); 70.6–70.4 (CH_2, C-22/C-23); 69.7 (CH_2, C-24); 68.3 (CH_2, C-21); 55.7 (CH, C-14); 53.4 (CH, C-12); 44.1 (CH_2, C-25); 39.4 (CH_2, C-20); 38.5 ($2CH_2$, C-8/C-18); 31.3 (CH_2, C-11); 30.7 (CH_2, C-15); 29.7–29.1 (CH_2, C-9/C-17); 28.4 (CH_3, Boc); 23.1 (CH_2, C-16); 22.7 (CH_2, C-10); 22.4 (CH_3, ^{i}Pr); 22.1 (CH_3, ^{i}Pr). HRMS (FAB$^+$) *m/z*: $[M + H]^+$ calcd. For $C_{55}H_{82}N_9O_{15}$: 1108.5925; found: 1108.5971. $[\alpha]_D^{25}$ = +10.7 (c = 0.13, $CHCl_3$).

Synthesis of AMB-NBD2 (6): To a solution of **18** (60 mg, 0.054 mmol) in anhydrous CH_2Cl_2 (5 mL) at −78 °C, was added BCl_3 (340 μL,

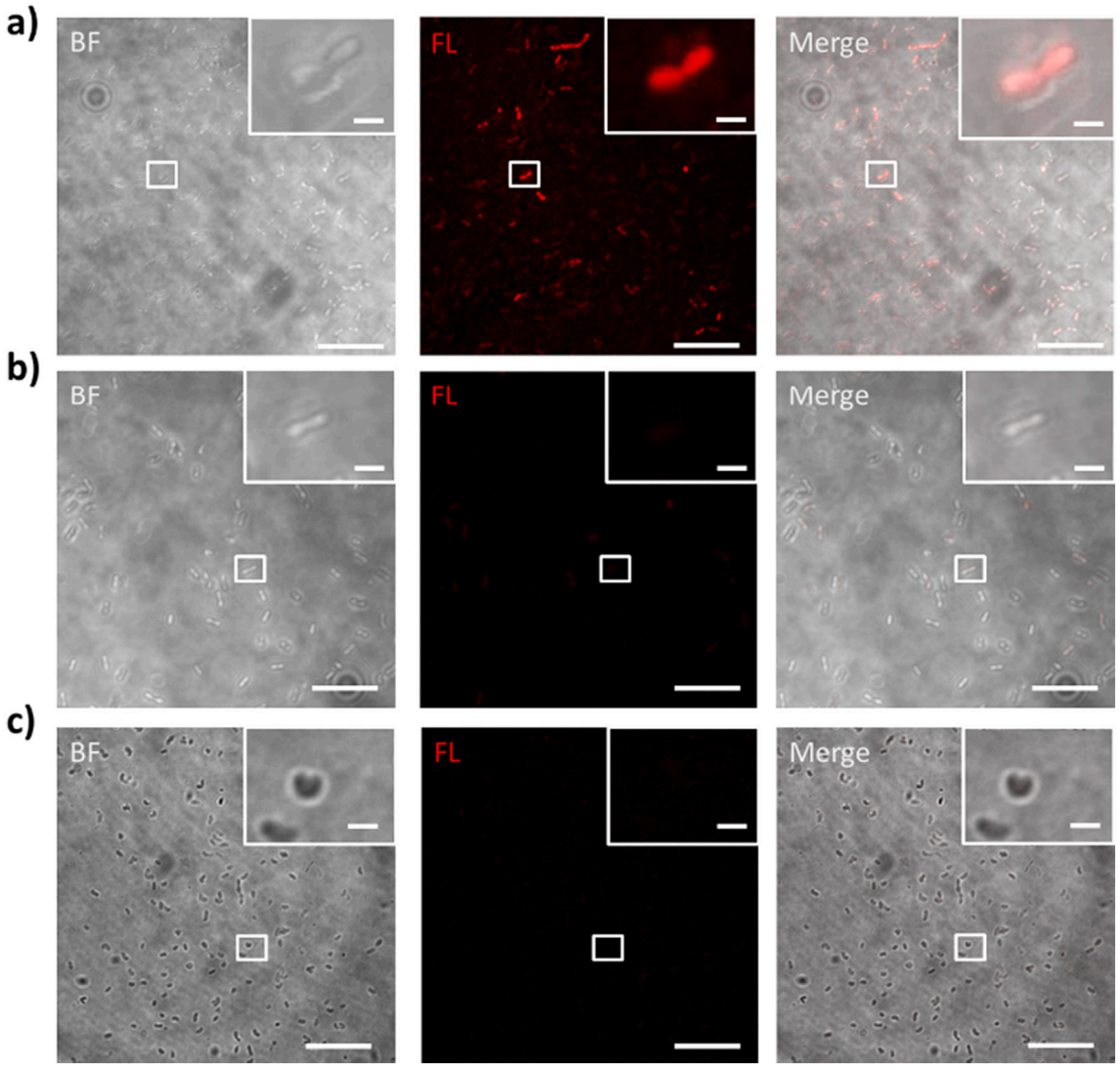

Fig. 5. Epifluorescence microscopy images observed at 1000×. a) *A. salmonicida* FstC(+) (VT45.1Δ*entB)*. b) *A. salmonicida* FstC(−) (VT45.1Δ*entB*Δ*fstC)*. c) *Vibrio anguillarum*. Scale bar: 10 μm (full view) or 1 μm (enlarged view). All bacteria tested were precultured in CM9 minimal medium, with iron chelator EDDHA at 5 μM, and treated with 6.5 μM of **AMB-SRB** (**7**) for 12 h at 25 °C. Left: Phase contrast (BF), middle: fluorescence channel (FL), right: merged images.

1 M in CH_2Cl_2), and the mixture was stirred overnight at −40 °C. Then, 5 mL of water was added to quench the reaction and concentrated under reduced pressure. The residue was purified by HPLC using a Discovery HS F5 (100 × 4.6 mm, 5 μm) column with a mobile phase consisting of a gradient of 10% CH_3CN to 100% in H_2O (*v*/v), each containing 0.1% TFA, for 20 min, at a flow rate of 2 mL/min (injected volume 1 mL; detection 254 nm, retention time 18 min), to give **6** (28 mg, 0.033 mmol, 62%) as an orange oil. ^{1}H NMR (500 MHz, CD_3OD): δ 8.45 (d, J = 8.7 Hz, 1H, H-30); 7.22–7.12 (m, 2H, H-6/6′); 6.93–6.85 (m, 2H, H-4/4′); 6.72–6.63 (m, 2H, H-5/5′); 6.35 (d, J = 8.7 Hz, 1H, H-31); 4.33 (t, J = 6.7 Hz, 1H, H-14); 3.89 (t, J = 6.3 Hz, 1H, H-12); 3.79 (t, J = 5.5 Hz, 2H, H-21); 3.75–3.67 (m, 2H, H-24); 3.66–3.57 (m, 4H, H-22/H-23);3.48 (t, J = 5.7 Hz, 2H, H-25); 3.42–3.18 (m, 6H, H-8/H-18/H-20); 1.94–1.60 (m, 8H, H-9/H-11/H-15/H-17); 1.52–1.36 (m, 4H, H-10/H-16). ^{13}C NMR (125 MHz, CD_3OD): δ 173.6 (CO, C-13); 171.4 (2 x CO, C-7/7′); 170.0 (CO, C-19); 150.1 (2C, C-2/2′); 147.3 (2C, C-3/3′); 145.8–145.4 (C, C-27-28); 138.4 (CH, C-30); 123.3 (2C, C-1/1′); 119.6 (2CH, C-4/4′); 118.6 (2C, C-5/5′); 117.2 (C, C-29); 116.7 (2CH, C-6/6′); 114.9 (C, C-26); 100.1 (CH, C-31); 71.6–71.3 (CH_2, C-22/C-23); 70.5 (CH_2, C-24); 69.8 (CH_2, C-21); 54.9 (CH, C-14); 54.2 (CH, C-12); 44.7 (CH_2, C-25); 40.3–40.0 (3CH_2, C-8/C-18/C-20); 32.9 (CH_2, C-11); 32.4 (CH_2, C-15); 30.1 (2CH_2, C-9/C-17); 24.1 (CH_2, C-16); 23.1 (CH_2, C-10). HRMS (ESI$^+$) *m/z*: $[M + H]^+$ calcd. For $C_{38}H_{50}N_9O_{13}$: 840.3523; found: 840.3526. $[\alpha]_D^{25}$ = +6.9 (c = 0.10, CH_3OH).

Synthesis of amonabactin analogue 4- sulforhodamine B conjugate (AMB-SRB) (7).

Synthesis of 19: A solution of cysteamine (200 mg, 2.59 mmol) and trityl chloride (725 mg, 2.60 mmol) in anhydrous DMF (10 mL) was stirred at room temperature overnight. Then, 20 mL of water was added, and the mixture was extracted with EtOAc (2x30mL), washed with water and brine, dried with $MgSO_4$, filtered, and concentrated under reduced pressure. The residue was purified by silica gel column chromatography eluting with MeOH:CH_2Cl_2 (4:96) to obtain **17** (505 mg, 1.58 mmol, 61%) as a yellow oil. ^{1}H NMR (300 MHz, $CDCl_3$): δ 7.48–7.41 (m, 6H, Trt); 7.33–7.18 (m, 9H, Trt); 2.58 (t, J = 6.7 Hz, 2H, CH_2-NH_2); 2.36 (t, J = 6.7 Hz, 2H, CH_2-STrt); 2.03 (s, 2H, NH_2). ^{13}C NMR (75 MHz, $CDCl_3$): δ 145.0 (C, Trt); 129.7 (CH, Trt); 128.0 (CH, Trt); 126.8 (CH, Trt); 66.7 (C, Trt); 40.9 (CH_2-NH_2); 35.8 (CH_2-STrt). HRMS (ESI$^+$) *m/z*: $[M + H]^+$ calcd. For $C_{21}H_{22}NS$: 320.1467; found: 320.1466.

Synthesis of 20: To a solution of **8** (180 mg, 0.32 mmol) in CH_2Cl_2 (5 mL) was added a solution of **19** (110 mg, 0.34 mmol) in CH_2Cl_2 (5 mL) and DIPEA (120 μL, 0.69 mmol), and the mixture was stirred at room temperature for 4 h. Then, it was concentrated under reduced pressure, and the residue was purified by silica gel column

Table 1
Results of the observation under fluorescence microscopy of the different strains used to test the specificity of the **AMB-SRB** (**7**) probe. The percentages indicate the similarity of FstC transporter compared to *A. salmonicida* subsp. *salmonicida*. [15].

Species	Fluorescence with AMB-SRB (7)	FstC Aminoacidic similarity (%)	*fstC* Nucleotidic similarity (%)
Aeromonas salmonicida subsp. *salmonicida*	+	100	100
A. salmonicida subsp. *pectinolytica*	+	97.41	98.48
A. salmonicida subsp. *achromogenes*	+	99.85	99.80
A.hydrophila	+	94.37	91.65
A. sobria	+	60.94	69.30
Vibrio anguillarum	−	NP	NP
Photobacterium damselae subsp. *piscicida*	−	NP	NP

(+) = strains showed fluorescence when they were cultured with the probe **7**. (−) = absence of fluorescence when the strain was cultured with the probe **7**. NP = not present.

chromatography eluting with hexane:EtOAc (3:2) to obtain **20** (228 mg, 0.30 mmol, 93%) as a yellow oil. ^{1}H NMR (400 MHz, $CDCl_3$): δ 8.07 (t, J = 5.7 Hz, 1H, NH-7); 7.68 (dd, J = 8.0, 1.5 Hz, 1H, H-6); 7.42–7.36 (m, 6H, Trt); 7.31–7.24 (m, 6H, Trt); 7.22–7.16 (m, 3H, Trt); 7.06 (t, J = 8.0 Hz, 1H, H-5); 7.00 (dd, J = 8.0, 1.5 Hz, 1H, H-4); 6.27 (t, J = 5.3 Hz, 1H, NH-13); 5.21 (d, J = 6.7 Hz, 1H, NH-Boc); 4.66 (hept, J = 6.2 Hz, 1H, ^{i}Pr); 4.55 (hept, J = 6.2 Hz, 1H, ^{i}Pr); 4.01–3.92 (m, 1H, H-12); 3.51–3.32 (m, 2H, H-8); 3.12–3.00 (m, 2H, H-14); 2.39 (sext, J = 5.5 Hz 2H, H-15); 1.90–1.79 (m, 2H, H-11); 1.69–1.55 (m, 2H, H-9); 1.39 (s, 9H, Boc); 1.36 (d, J = 6.2 Hz, 6H, ^{i}Pr); 1.28 (d, J = 6.2 Hz, 6H, ^{i}Pr). ^{13}C NMR (100 MHz, $CDCl_3$): δ 171.9 (CO, C-13); 166.0 (CO, C-7); 155.7 (CO, Boc); 150.8 (C, C-2); 146.0 (C, C-3); 144.7 (C, Trt); 129.6 (CH, Trt); 128.4 (C, C-1); 128.0 (CH, Trt); 126.8 (CH, Trt); 123,7 (CH, C-4); 123.0 (CH, C-5); 118.3 (CH, C-6); 79.9 (C, Boc); 76.3 (CH, ^{i}Pr); 71.1 (CH, ^{i}Pr); 66.8 (C, Trt); 54.5 (CH, C-12); 38.8 (CH_2, C-14); 38.2 (CH_2, C-8); 31.8 (CH_2, C-15); 29.7 (CH_2, C-11); 29.5 (CH_2, C-9); 28.3 (CH_3, Boc); 22.8 (CH_2, C-10); 22.4 (CH_3, ^{i}Pr); 22.1(CH_3, ^{i}Pr). HRMS (ESI$^+$) m/z: [M + H]$^+$ calcd. For $C_{45}H_{58}N_3O_6S$: 768.4041; found: 768.4045. $[\alpha]_D^{25}$ = +32.3 (c = 0.17, $CHCl_3$).

Synthesis of 21: A solution of **20** (220 mg, 0.29 mmol) in 5 mL of a mixture of TFA/CH_2Cl_2 (1:9) was stirred at room temperature for 90 min. Then, the mixture was concentrated under reduced pressure to obtain **21** (190 mg, 0.29 mmol, quant.) as a yellow oil. It was used in next step without purification.

Synthesis of 23: To a solution of **22** (180 mg, 0.29 mmol) in CH_2Cl_2 (5 mL) was added a solution of **21** (200 mg, 0.30 mmol) in CH_2Cl_2 (5 mL) and DIPEA (100 μL, 0.58 mmol), and the mixture was stirred at room temperature for 4 h. Then, it was concentrated under reduced pressure, and the residue was purified by silica gel column chromatography eluting with EtOAc to obtain **23** (213 mg, 0.18 mmol, 64%) as a yellow oil. ^{1}H NMR (400 MHz, $CDCl_3$): δ 8.82 (t, J = 5.3 Hz, 1H, NH); 8.08 (t, J = 5.7 Hz, 1H, NH); 7.66–7.60 (m, 2H, H-6/6′); 7.41–7.35 (m, 6H, Trt); 7.28–7.21 (m, 6H, Trt); 7.20–7.14 (m, 4H, Trt/NH); 7.10–6.97 (m, 5H, H-4/4'/H-5/5'/NH); 6.88–6.80 (m, 1H, NH); 5.63 (d, J = 7.4 Hz, 1H, NH-Boc); 4.69 (2 x hept, J = 6.2 Hz, 2H, ^{i}Pr); 4.54 (2 x hept, J = 6.2 Hz, 2H, ^{i}Pr); 4.363 (m, 1H, H-14); 4.11–4.04 (m, 3H, H-20/H-12); 3.50–3.25 (m, 6H, H-8/H-18/H-22); 2.39 (t, J = 6.9 Hz, 2H, H-23); 1.94–1.83 (m, 8H, H-19/H-11/H-15/H-17); 1.39 (s, 9H, Boc); 1.37–1.31 (m, 16H, H-10/H-16/ ^{i}Pr); 1.29–1.23 (m, 12H, ^{i}Pr). ^{13}C NMR (100 MHz, $CDCl_3$): δ 172.6/171.5169.0 (3 x CO, C-19/C-21/C-15/ C-21); 166.2 (CO, C-7/7′); 156.0 (CO, Boc); 150.9 (C, C-2/2′); 146.9/146.0 (C, C-3/3′); 144.7 (C, Trt); 129.6 (CH, Trt); 128.4/127.5 (C, C-1/1′); 127.9 (CH, Trt); 126.7 (CH, Trt); 123.8/123.6 (CH, C-4/4′); 122.9/122.7 (CH, C-5/5′); 119.4/118.3 (CH, C-6/8′); 79.9 (C, Boc); 76.6/76.3 (CH, ^{i}Pr); 71.5/71.1 (CH, ^{i}Pr); 66.7 (C, Trt); 54.8 (CH, C-14); 53.2 (CH, C-12); 43.9 (CH_2, C-8); 39.0 (CH_2, C-22);38.7 (CH_2, C-20); 38.6 (CH_2, C-10); 31.9 (CH_2, C-17); 31.7 (CH_2, C-23); 31.2 (CH_2, C-13); 29.4 (CH_2, C-19); 28.7 (CH_2, C-11); 28.4 (CH_3, Boc); 22.7 (CH_2, C-18/C-12); 22.4 (CH_3, ^{i}Pr); 22.1(CH_3, ^{i}Pr). HRMS (ESI$^+$) m/z: [M + Na]$^+$ calcd. For $C_{66}H_{88}N_6O_{11}SNa$: 1195.6124; found: 1195.6124. $[\alpha]_D^{25}$ = +19.8 (c = 0.12, $CHCl_3$).

Synthesis of 24: To a solution of **23** (180 mg, 0.15 mmol) in anhydrous CH_2Cl_2 (5 mL) at −78 °C was added BCl_3 (1.5 mL, 1 M in CH_2Cl_2), and the mixture was stirred overnight at −40 °C. Then, 5 mL of water was added to quench the reaction and concentrated under reduced pressure. The residue was purified by HPLC using a Discovery HS F5 (100 × 4.6 mm, 5 μm) column with a mobile phase consisting of a gradient of 10% CH_3CN to 100% in H_2O (*v*/v), each containing 0.1% TFA, for 15 min, at a flow rate of 2 mL/min (injected volume 1 mL;

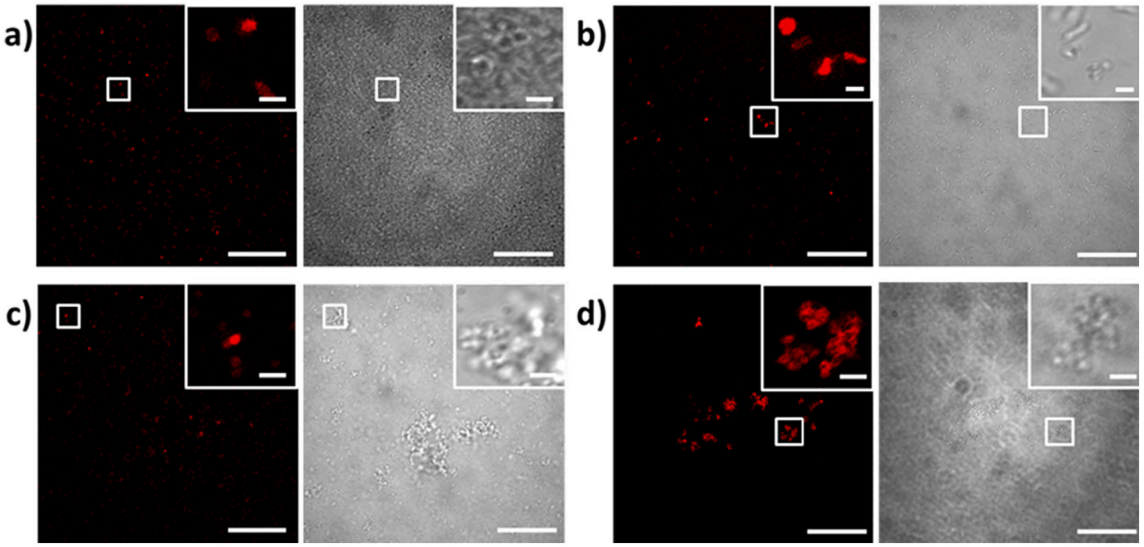

Fig. 6. Epifluorescence microscopy images observed at 1000×. a) *A. hydrophila*. b) *A. sobria*. c) *A. salmonicida* subsp. *pectinolytica*. d) *A. salmonicida* subsp. *achromogenes*. Scale bar: 10 μm (full view) or 1 μm (enlarged view). All bacteria tested were precultured in CM9 minimal medium, with iron chelator EDDHA at 5 μM, and treated with 6.5 μM of **AMB-SRB** (**7**) for 12 h at 25 °C. Left: fluorescence channel; right: Phase contrast.

detection 254 nm, retention time 12 min), to give **24** (76 mg, 0.11 mmol, 75%) as a white solid.

^{1}H NMR (500 MHz, CD_3OD): δ 7.27 (dd, J = 8.0, 1.5 Hz, 1H, H-6); 7.20 (dd, J = 8.0, 1.5 Hz, 1H, H-6′); 6.95 (dd, J = 8.0, 1.5 Hz, 1H, H-4); 6.92 (dd, J = 8.0, 1.5 Hz, 1H, H-4′); 6.73 (2 t, J = 8.0 Hz, 2H, H-5/H-5′); 4.31 (dd, J = 8.1, 5.7 Hz, 1H, H-12); 4.04 (d, J = 2.8 Hz, 2H, H-20); 3.86 (t, 1H, J = 6.7 Hz, H-14); 3.41–3.34 (m, 4H, H-8/H-18); 3.26 (t, J = 6.8 Hz, 2H, H-22); 2.58 (t, J = 6.8 Hz, 2H, H-23); 1.92–1.71 (m, 4H, H-11/H-15); 1.69-.52 (m, 4H, H-9/H-17); 1.51–1.38 (m, 4H, H-10/H-16). ^{13}C NMR (125 MHz, CD_3OD): δ 173.9 (CO, C-21); 171.8 (CO, C-7); 171.4 (CO, C-9); 170.0 (CO, C-15); 150.0 (C, C-2); 147.3 (C, C-3); 119.8 (CH, C-4); 119.6 (CH, C-5); 118.7/ 119.2 (CH, C-6); 116.,9 (C, C-1); 55.1 (CH, C-16); 54.2 (CH, C-14); 43.8 (CH_2, C-8/C-22); 40.0 (CH_2, C-20); 39.6 (CH_2, C-10); 32.8 (CH_2, C-17); 32.2 (CH_2, C-13); 30.1 (CH_2, C-19); 29.9 (CH_2, C-11); 24.5 (CH_2, C-23); 24.2 (CH_2, C-18); 22.8 (CH_2, C-12). HRMS (ESI$^+$) m/z: $[M + H]^+$ calcd. For $C_{30}H_{43}N_6O_9S$: 663.2807; found: 663.2796. $[\alpha]_D^{25}$ = +11.0 (c = 0.13, CH_3OH).

Synthesis of 25: To a solution of 2-(2-aminoethoxy)ethanol (450 μL, 4.49 mmol), and di-*tert*-butyl dicarbonate (Boc_2O) (1 g, 4.57 mmol) in anhydrous CH_2Cl_2, was added DIPEA (860 μL, 4.94 mmol), and the mixture was stirred overnight at room temperature. Then, it was concentrated under reduced pressure, and the residue was redisolved in EtOAc (15 mL), washed with water and brine, dried with $MgSO_4$, filtered and concentrated under reduced pressure, to obtain **25** (906 mg, 4.41 mmol, 98%) as a colourless oil. ^{1}H NMR (300 MHz, $CDCl_3$): δ 5.15 (brs, 1H, NH-Boc); 3.70 (t, J = 4.5 Hz, 2H, H-1); 3.56–3.47 (m, 4H, H-2/H-3); 3.29 (q, J = 5.3 Hz, 2H, H-4); 2.76 (s, 1H, OH); 1.41 (s, 9H, Boc). ^{13}C NMR (75 MHz, $CDCl_3$): δ 156.2 (CO, Boc); 79.4 (C, Boc); 72.3 (CH_2, C-3); 70.4 (CH_2, C-2); 61.7 (CH_2, C-1); 40.5 (CH_2, C-4); 28.5 (CH_3, Boc). HRMS (ESI$^+$) m/z: $[M + Na]^+$ calcd. For $C_9H_{19}NO_4Na$: 228.1206; found: 228.1207.

Synthesis of 26: To a solution of PPh_3 (716 mg, 2.73 mmol) in anhydrous THF (8 mL) at −78 °C, was added sequentially diethyl azodicarboxylate (DEAD) (435 μL, 2.73 mmol), a solution of **25** (616 mg, 3.00 mmol) in 4 mL of anhydrous tetrahydrofuran (THF), neopentyl alcohol (120 mg, 1.36 mmol), and maleimide (265 mg, 2.73 mmol). After 5 min, the reaction was allowed to reach room temperature, and was stirred overnight. Then, it was concentrated under reduced pressure, and the residue was purified by silica gel column chromatography eluting with hexane:EtOAc (2:1) to obtain **26** (630 mg, 2.21 mmol, 81%) as a white solid. ^{1}H NMR (300 MHz, $CDCl_3$): δ 6.66 (s, 2H, H-1); 4.92 (brs, 1H, NH-Boc); 3.70 (t, J = 5.5 Hz, 2H, H-3); 3.53 (t, J = 5.5 Hz, 2H, H-4); 3.42 (t, J = 5.2 Hz, 2H, H-5); 3.18 (q, J = 5.2 Hz, 2H, H-6); 1.41 (s, 9H, Boc). ^{13}C NMR (75 MHz, $CDCl_3$): δ 170.7 (CO, C-2); 155.9 (CO, Boc); 134.2 (CH, C-1); 79.2 (C, Boc); 69.8 (CH_2, C-5); 67.7 (CH_2, C-4); 40.3 (CH_2, C-6); 37.2 (CH_2, C-3); 28.4 (CH_3, Boc). HRMS (ESI$^+$) m/z: $[M + Na]^+$ calcd. For $C_{13}H_{20}N_2O_5Na$: 307.1264; found: 307.1257.

Synthesis of 27: A solution of **26** (220 mg, 0.29 mmol) in 5 mL of a mixture of TFA/CH_2Cl_2 (1:9) was stirred at room temperature for 90 min. Then, the mixture was concentrated under reduced pressure to obtain **27** (205 mg, 0.29 mmol, quant.) as a white solid. It was used in next step without purification.

Synthesis of 28: To a solution of sulforhodamine B acid chloride (30 mg, 0.05 mmol) and **27** (31 mg, 0.01 mmol) in anhydrous dimethylformamide (DMF) (4 mL), was added Et_3N (30 μL, 0.02 mmol), and the mixture was stirred overnight at room temperature. Then, it was concentrated under reduced pressure, and the residue was purified by HPLC using a Atlantis dC18 (100 × 10 mm, 5 μm) column with a mobile phase consisting on a gradient of 10% CH_3CN to 100% in H_2O (*v*/v), each containing 0.1% TFA, for 15 min, at a flow rate of 2 mL/min (injected volume 1 mL; detection 254 nm, retention time 10 min), to give **28** (28 mg, 0.04 mmol, 38%) as a purple solid. ^{1}H NMR (500 MHz, CD_3OD): δ 8.67 (d, J = 1.8 Hz, 1H, H-8); 8.13 (dd, J = 7.9, 1.8 Hz, 1H, H-12); 7.54 (d, J = 7.9 Hz, 1H, H-11); 7.14 (d, J = 9.6 Hz, 2H, H-19); 7.04 (dd, J = 9.5, 2.5 Hz, 2H, H-18); 6.96 (d, J = 2.5 Hz, 2H, H-16); 6.84 (s, 2H, H-1); 3.72–3.66 (m, 10H, H-20/H-3); 3.57 (t, J = 5.5 Hz, 2H, H-4); 3.53 (t, J = 5.5 Hz, 2H, H-5); 3.19 (t, J = 5.5 Hz, 2H, H-6); 1.32 (t, J = 7.1 Hz, 12H, H-21). ^{13}C NMR (125 MHz, CD_3OD): δ 172.5 (CO, C-2); 159.4 (C, C-14); 157.8 (C, C-13); 157.1 (C, C-17); 147.1 (C, C-7); 144.2 (C, C-9); 135.5 (CH, C-1); 135.4 (C, C-10); 133.7 (CH, C-19); 132.4 (CH, C-11); 129.3 (CH, C-12); 127.6 (CH, C-8); 115.3 (C, C-14); 115.1 (CH, C-18); 96.9 (CH, C-16); 70.2 (CH_2, C-5); 69.9 (CH_2, C-4); 46.8 (CH_2, C-20); 44.0 (CH_2, C-6); 38.1 (CH_2, C-3); 12.8 (CH_3, C-21). HRMS (ESI$^+$) m/z: $[M + H]^+$ calcd. For $C_{35}H_{41}N_4O_9S_2$: 725.2309; found: 725.2305.

Synthesis of AMB-SRB (7): To a solution of **24** (4.5 mg, 0.007 mmol) in 2 mL of CH_3CN: Phosphate buffer (0.1 M, pH = 7) (2:1) mixture, was added a solution of **28** (5 mg, 0.007 mmol) in 2 mL of the same mixture and it was stirred at room temperature for 2 h. Then, it was concentrated under reduced pressure, and the residue was purified by HPLC using a Discovery HS F5 (100 × 4.6 mm, 5 μm) column with a mobile phase consisting on a gradient of 10% CH_3CN to 100% in H_2O (*v*/v), each containing 0.1% TFA, for 15 min, at a flow rate of 2 mL/min (injected volume 1 mL; detection 254 nm, retention time 14 min), to to give **7** as mixture of two epimers at C24 (7.5 mg, 0.005 mmol, 80%) as a purple solid. ^{1}H NMR (500 MHz, CD_3OD): δ 8.72/8.71 (d/d, J = 1.8 Hz, 1H, Aromatic H SRB); 8.11/8.10 (d/d, J = 8.0 Hz, 1H, Aromatic H SRB); 7.51 (d, J = 8.0 Hz, 1H, Aromatic H SRB); 7.20 (d, J = 8.0 Hz, 1H, H-6); 7.11–7.06 (m, 3H, H-6′/ Aromatic H SRB); 6.98–6.90 (m, 3H, H-4/ Aromatic H SRB); 6.87 (d, J = 8.0 Hz, 1H, H-4′); 6.84–6.79 (m, 2H, Aromatic H SRB); 6.67 (epimers, t/t, J = 8.0 Hz, 1H, H-5); 6.58 (epimers t/t, J = 8.0 Hz, 1H, H-5′); 4.34 (dd, J = 8.4, 5.4 Hz, 1H, H-12); 4.00–3.92 (m, 3H, H-20/H-24); 3.89 (m, 1H, H-14); 3.70–3.55 (m, 12H, H-29/H-30/ $CH_3\underline{CH_2}N$ SRB); 3.54–3.48 (m, 2H, H-28); 3.48 (m, 2H, H-22); 3.28–3.12 (m, 5H, H-8/H-18/H-31/H-25a); 3.01/2.98 (epimers, dd/dd, J = 14.6, 6.0 Hz, H-23a); 2.81 (m, 1H, H-23b); 2.55/2.54 (epimers, dd/dd, 11.3, 3.8 Hz 1H, H-25b); 1.96–1.64 (m, 4H, H 11/H-15); 1.61 1.51 (m, 4H, H-9/H-17); 1.49–1.38 (m, 4H, H-10/H-16); 1.26 (t, J = 7.1 Hz, 12H, $\underline{CH_3}CH_2N$ SRB). ^{13}C NMR (125 MHz, CD_3OD): δ 179.0/178.9 (epimers CO, C-26/C-27); 177.1/177.0 (epimers, CO, C-27), 173.9 (CO, C-21); 171.7/171.7/171.5 (epimers CO, C-7 and C7'); 170.2/170.1 (epimers CO, C-13); 170.1 (CO, C-19); 159.2/157.6/157.0 (3C, Aromatic C SRB); 150.3/150.1 (C, C-2/2′); 147.3 (C, C-3/3′); 147.1/143.9/135.5 (3C, Aromatic C SRB); 133.6/132.6/129.5/127.7 (4CH, Aromatic C SRB); 119.8 (CH, C-4/4′); 119.5 (CH, C-5/5′); 119.2/118.7 (CH, C-6/6′); 116.6 (C, C-1/1′); 115.2 (C, Aromatic C SRB); 115.0/96.9 (2CH, Aromatic C SRB); 70.1/68.1 (four signals, epimers, $2CH_2$, C-29/C-30); 55.1 (two signals, epimers, CH, C-12); 54.3 (two signals, epimers, CH, C-14); 46.8 (CH_2, $CH_3\underline{CH_2}N$ SRB); 44.2 (CH_2, C-31); 43.7 (CH_2, C-8); 40.6 (CH, C-24); 40.0 (CH_2, C-22); 39.9 (CH_2, C-20); 39.6/39.5/39.4/37.1 ($3CH_2$, C-8/C-18/ -25/C-28); 32.8/32.2/31.7 ($3CH_2$, C-9/C-17/C-23); 29.9/29.8 ($2CH_2$, C-11/C-15); 24.2/22.9 ($2CH_2$, C-10/C-16); 12.9 (CH_3, $\underline{CH_3}CH_2N$ SRB). HRMS (ESI$^+$) m/z: $[M + H]^+$ calcd. For $C_{65}H_{83}N_{10}O_{18}S_3$: 1387.5043; found: 1387.5026. $[\alpha]_D^{25}$ = +6.7 (c = 0.10, CH_3OH).

Synthesis of AMB-SRB ferric complex: To 0.5 mL of a AMB-SRB (**7**) (2 mg, 1.44 μmol) solution in a MeOH:H_2O (1:1) was added 0.5 mL of a $Fe(acac)_3$ (1 mg, 2.83 μmol) solution in MeOH:H_2O (1:1). The mixture was stirred at room temperature for 12 h. After that time, an aliquot of the resulting mixture was analyzed by HRMS (ESI$^-$). HRMS (ESI$^-$): m/z 1438.4011 (calculated for $C_{65}H_{78}FeN_{10}O_{18}S_3$, m/z 1438.4013).

3. Results and discussion

3.1. Synthesis of fluorescent conjugates

As starting point, we selected **3** as the most simplified analogue of AMBs that keeps the siderophore activity, and the fluorophore 4-chloro-7-nitrobenzofurazan (NBD) which has been already used to be conjugated with other siderophore derivatives such as pyochelin, a phenolate/thiazoline siderophore. Pyochelin derivatives conjugated with NBD successfully labelled *Pseudomonas aeruginosa*.[18] Even though the static quenching on NBD fluorophore is produced when this fluorophore is conjugated to hydroxamate-type siderophores,[17],[23] there was no

reported information about its behaviour with catechol-type siderophores.

As outlined in Scheme 1, synthesis of the first conjugate **AMB-NBD1** (**5**) started with the preparation of the building block **8**, from 2,3-dihydroxybenzoic acid and N^{α}-Boc-L-Lys, which was converted to the convenient protected analogue amonabactin **9**, using a previous described synthetic procedure,[15] and subsequent deprotection of *tert*-butyloxycarbonyl (Boc) group to obtain **10**. In a parallel procedure, the NBD-spacer arm **12** was obtained by coupling the commercially available *tert*-butyl 12-amino-4,7,10-trioxadodecanoate with NBD, followed by removal of *tert*-butyl group and subsequent activation of the carboxylic acid with *N*-hydroxysuccinimide (NHS). Finally, coupling of **10** and **12**, followed by removal of isopropyl protecting groups afforded **AMB-NBD1** (**5**).

The internalization of **5** was studied by bacterial growth assays with the mutant strain *A. salmonicida* VT45.1Δ*entB* under iron starvation. This strain cannot biosynthesize endogenous siderophores (acinetobatin or AMBs) due to the mutation of *entB* gene, key to the synthesis of the catechol group. Therefore, this strain requires the addition of exogenous siderophores to grow under iron limitation. As shown in Fig. 2, although this *A. salmonicida* strain was able to grow with the addition of amonabactin analogue **3**, the conjugate **AMB-NBD1** (**5**) failed to induce bacterial growth at all concentrations tested. These results suggest that the presence of a free amine group at C14 position is crucial for the molecular recognition of the conjugate by the OMT FstC to be internalized by the cells of *A. salmonicida*.

For this reason, we decided to synthetize a second conjugate AMB-NBD2 (**6**) bearing a free amino group at C14 and connecting the cargo through a carboxylic acid functionality at C12 position, mimicking the structures of natural AMBs, which have an amino acid moiety (D-Phe or D-Trp) attached to that position. Thus, a second NBD-spacer arm **14** was synthetized by coupling NBD with commercially available *N*-Boc-2,2′-(ethylenedioxy)-diethylamine, followed by removal of the Boc group to give **15**. Then, conjugation of **15** with building block **8** afforded the intermediate **16** which was submitted to deprotection of the Boc protection group, affording **17**, and subsequent coupling again with **8** to give **18**. Finally, total deprotection of the ^{i}Pr and Boc groups with BCl_3 of **18** furnished the required **AMB-NBD2** (**6**) (Scheme 1).

In this case, bacterial growth promotion assays with the same mutant strain of *A. salmonicida* showed that conjugate **6** restored the growth at two of the concentration tested and, in a concentration-dependent manner (Fig. 2). It is worth mentioning that the growth promotion of **6** was lower than AMB analogue **3**. A similar trend was already observed for natural AMBs in relation to their simplified analogues **3** and **4**.[15].

These results seem to indicate the crucial role of the existence of a free amine group at C14 for molecular recognition of amonabactin analogues by FstC and the presence of a carboxylic acid functionality at C12 as a suitable position for substitution. As expected, modifications in the siderophore structure, even though keeping the key elements for recognition, cause a decrease in the biological activity. However, when we incubated the mutant strain *A. salmonicida* VT45.1Δ*entB* with **AMB-NBD2** (**6**) and examined the bacterial cells by epifluorescence microscopy, we were unable to observe any fluorescence in the bacterial cells. This lack of fluorescent labelling was attributed to fluorophore quenching. Indeed, Fe(III) titration assays (Fig. 3) showed that fluorescence emission of **6** was quenched due to the Fe(III) complexation process of the siderophore moiety of the conjugate. A similar process was reported with analogues of the hydroxamate-type siderophores deferoxamine[24] and ferrichrome[23] labelled with NBD. The same effect was observed with other fluorophores and even with natural fluorescent siderophores like pyoverdine.[25].

The positive results reported for a pyochelin-NBD fluorescent probe seems to be an exception probably due to its particular intrinsic fluorescence properties.[18].

The fact that **AMB-NBD2** (**6**) is fluorescent only when unferrated indicates its possible application as a probe to follow iron removal from a siderophore or as a Fe^{3+} sensor. A NBD-desferrioxamine B probe, which displayed a similar behaviour, was applied to study iron uptake in plants.[26].

The quenching process observed with NBD led us to choose another fluorophore to design an AMB-based fluorescent probe. Thus, inspired by Shanzer et al. work,[17] we selected sulforhodamine B (SRB) as fluorophore. Although the size of SRB is bigger than NBD, SRB has a higher fluorescence intensity and polarity. A new synthetic route had to be designed for the preparation of the third conjugate AMB-SRB (**7**) due to the probable decomposition of the SRB moiety in the presence of BCl_3 during the deprotection step. In this way, we decided to prepare a "clickable" AMB-thiol **24** which could be easily linked to maleimide containing ligands for conjugation not only with fluorophore arms but also with antibiotics to develop the Trojan horse strategy with this type of compounds. In this case, we prepared a conjugate of an amonabactin analogue similar to **4**, which incorporates a 15 atoms length linker between the two catecholamide moieties, because we had previously found that **4** with this linker has higher siderophore activity than **3** bearing a shorter linker (12 atoms linker length).[15].

As shown in Scheme 2, synthesis of **AMB-SRB** (**7**) started with the thiol protection of cysteamine with the trityl (Trt) group, affording amine **19**, which was coupled with activated building block **8** to yield **20**. Subsequently, removal of the Boc group in **20** gave amine **21**. Next, building block **22**, which was prepared from 2,3 dihydroxy benzoic acid (2,3-DHBA), N^{α}-Boc-L-Lys and N^{α}-Cbz-Gly using a previous described procedure,[15] was coupled with **21** to afford **23**. Treatment of **23** with BCl_3 allowed the removal of all protecting groups to give AMB-thiol **24**. In a parallel procedure, commercially available 2-(2-aminoethoxy) ethanol was protected with Boc group to afford carbamate **25**, which was coupled to maleimide under Mitsunobu reaction conditions to yield **26**.[27].

Removal of the Boc protecting group in carbamate maleimide **26** gave intermediate **27**, which was coupled with sulforhodamine B acid chloride in DMF to furnish the SRB-spacer arm **28**.[28] Finally, **28** and **24** were coupled in a CH_3CN/buffer mixture (2:1, phosphate buffer, pH 7, 0.1 M) to give, after purification by semi-preparative HPLC, the desired conjugate **AMB-SRB** (**7**).

The internalization of **AMB-SRB** (**7**) was firstly demonstrated by the growth induction observed in the mutant strain *A. salmonicida* VT45.1Δ*entB* under iron starvation after addition of **7** at two of the concentration tested (Fig. 4), suggesting that FstC must be the route of entry. This hypothesis was confirmed by testing the different conjugates with the FstC(−) mutant (VT45.1Δ*entB*Δ*fstC*), which could not internalize the probe (Fig. S1). These experiments provide evidence not only that AMB-SRB (**7**) is indeed acting as siderophore and delivering iron into the bacterial cells, but also that the OMT FstC is the route of entry. It is worth mentioning that the introduction of a bigger fluorophore implied a significant decrease of its biological activity probably due to a steric effect of the bulky SRB that hinders the molecular recognition by the OMT FstC. In fact, for compound **7** only the concentration of 13 μM stimulated bacterial growth significantly, showing ca. 56% activity of **4** or 41% activity of natural amonabactin P-750 (**2**) at the same concentration (Fig. 4). Further increase in **AMB-SRB** (**7**) concentration was not possible because the spectroscopic properties of the probe started to interfere with the measurement.

The influence of the size of the fluorophore was already reported in other siderophore-fluorescent probes. Ouchetto et al.[23] obtained similar results with a ferrichrome-NBD probe, which reduced its internalization rate, compared to the free siderophore, by around 80%.

It has been reported that ferrichrome analogues bound to various fluorophores also display reductions in their biological activity of up to 50%.[17] Other studies with enterobactin analogues also highlight the importance of the cargo size, although restrictions are variable and specific for each transporter and species.[29].

3.2. Coordination studies of Fe^{3+} with **AMB-SRB (7)**

The coordination chemistry of the natural amonabactins has been already reported and it has been elucidated using potentiometric and spectrophotometric titrations, circular dichroism, and mass spectrometry.[30] A study of the ferric complex of **AMB-SRB** (**7**) by mass spectrometry was carried out in order to demonstrate its formation. The (−)-HRESIMS of a solution of **AMB-SRB** (**7**), after addition of $Fe(acac)_3$, displays the presence of a prominent ion peak at *m/z* 1438.4011 (calculated for $C_{65}H_{78}FeN_{10}O_{18}S_3$ *m/z* 1438.4013), suggesting the existence of Fe in its structure. Moreover, presence of Fe was confirmed by the comparison of the experimental isotopic cluster observed around the ion peak at *m/z* 1438.4011 with the corresponding calculated isotopic cluster due to the presence of Fe^{+3} (Fig. S2). On the other hand, Fe(III) titration assays with **AMB-SRB** (**7**), in contrast with **AMB-NBD2 (6)**, showed that fluorescence emission of **7** was not quenched due to the Fe (III) complexation process of the siderophore moiety of the conjugate (Fig. S3).

3.3. Epifluorescence microscopy of **AMB-SRB (7)**

The ability of AMB-SRB (**7**) to target bacteria through the amonabactin uptake mechanism was tested via epifluorescence microscopy in *A. salmonicida* (Fig. 5). Incubation of VT45.1Δ*entB* strain (a FstC(+) strain carrying the amonabactin transporter FstC active) with conjugate **7** under iron starvation, showed that all bacterial cells were successfully labelled showing uniform distribution of the signal all over the shape of the cell (Fig. 5a). In contrast, the incubation of the FstC(−) mutant strain (VT45.1Δ*entB*Δ*fstC*) with **AMB-SRB** (**7**) did not induce fluorescence (Fig. 5b). Residual fluorescence spots were observed in some overexposed images, which was probably due to the presence of probe traces not removed by the washing procedure.

To assess the specificity of probe **7**, two common Gram-negative fish pathogenic bacteria, involved in severe infectious diseases in aquaculture, *Photobacterium damselae* subsp. *piscicida* and *Vibrio anguillarum* (both belonging to *Vibrionaceae* family) were subjected to fluorescent monitoring assays with **7**. *P. damselae* subsp. *piscicida* is responsible for photobacteriosis, a fish septicemia.[31] Piscibactin is the phenolate/thiazoline type siderophore involved in its iron uptake mechanism.[32] *V. anguillarum* is the aetiological agent of classical vibriosis, being the most common and also the most extensively studied *Vibrio* species in aquaculture.[8] Three different siderophore-mediated systems were described in this bacterium, two catecholate type, vanchrobactin[33] and anguibactin (bearing also a hydroxamate group)[34], and piscibactin.[35].

The development of a simple diagnostic method that could make it possible to distinguish between *A. salmonicida* and the other two Gram negative pathogenic bacteria would be very useful in the aquaculture industry. Thus, *Photobacterium damselae* subsp. *piscicida* and *V. anguillarum* were incubated with **AMB-SRB** (**7**) and investigated by epifluorescence microscopy. The results showed that neither *P. damselae* subsp. *piscicida* nor *V. anguillarum* were labelled by probe **7** (Fig. 5c, Table 1).

Since the outer membrane transporter FstC is conserved in most *Aeromonas* species [15], probe **7** could be used to detect *Aeromonas* spp., including the human pathogen *A. hydrophila*. To test this hypothesis, the fluorescent response of **AMB-SRB** (**7**) to several species belonging to the genus *Aeromonas* was also assayed. Incubation of *A. hydrophila*, *A. sobria*, *A. salmonicida* subsp. *pectinolytica*, and *A. salmonicida* subsp. *achromogenes* with **AMB-SRB** (**7**) induced fluorescence in all of them (Fig. 6, Table 1). Congruently, those bacteria containing a close homologue of the amonabactins OMT *fstC* in its genome showed fluorescence after being incubated with probe **7** (Table 1). Thus, probe **7** could be used as a diagnosis tool able to distinguish *A. salmonicida* from other common fish pathogenic bacteria such as *P. damselae* subsp. *piscicida* or *V. anguillarum*, and could also detect the presence of other *Aeromonas* spp.

4. Conclusion

In the present work, a new fluorescent probe by conjugation of the appropriate amonabactin analogue to sulforhodamine B (**AMB-SRB**, **7**) was designed and synthetized. We have demonstrated that **AMB-SRB** (**7**) is successfully taken up by *A. salmonicida* through its OMT protein FstC. These results indicate that probe **7** could be very useful as a molecular tool for studying amonabactin-dependent iron uptake mechanism in *Aeromonas* species, such as the fish pathogen *A. salmonicida*, the human pathogen *A. hydrophila* and other members of *Aeromonas*. The structure-activity relationships deduced from this analysis, such as the key role of the presence of a free amino group at C14, suggest that the intermediate **24** can be a promising candidate to vectorize antibiotics to apply the Trojan horse strategy to develop new antimicrobials against *A. salmonicida* or other *Aeromonas* species. Moreover, the ability to specifically distinguish *Aeromonas* cells from other fish pathogenic bacteria makes **AMB-SRB** (**7**) a potential tool for detection of *Aeromonas* spp. in fish farming environments through fluorescence assays.

Authors statements

C.J., J.R., M.B., M.L. conceived the experiments. J.C.-S., D.R.-V., conducted the experiments. All authors reviewed the manuscript.

Declaration of Competing Interest

The authors declare that they have no known competing financial interests or personal relationships that could have appeared to influence the work reported in this paper.

Acknowledgments

This work was supported by grants RTI2018-093634-B-C21/C22 from the State Agency for Research (AEI) of Spain, cofunded by the FEDER Programme from the European Union (MCIN/AEI/10.13039/501100011033/FEDER). M.B. was supported by grant PID2019-103891RJ-100 from MCIN/AEI (Spain). Work in University of Santiago de Compostela and University of A Coruña was also supported by grants GRC2018/018 and GRC2018/039, respectively, from Xunta de Galicia and BLUEBIOLAB (0474_BLUEBIOLAB_1_E), Programme INTERREG V A of Spain-Portugal (POCTEP). D.R-V. thanks Xunta de Galicia (Spain) for a predoctoral fellowship. J.C.-S. thanks to the FPU National Program (FPU16/02060) of the Spanish Ministry of Science, Innovation and Universities for a predoctoral fellowship.

Appendix A. Supplementary data

Supplementary data to this article can be found online at https://doi.org/10.1016/j.jinorgbio.2022.111743.

References

[1] A. Fernández-Bravo, M.J. Figueras, An Update on the Genus *Aeromonas*: Taxonomy, Epidemiology, and Pathogenicity, 2020, https://doi.org/10.3390/microorganisms8010129.
[2] S. Hoel, O. Vadstein, A.N. Jakobsen, The significance of mesophilic *Aeromonas* spp. in minimally processed ready-to-eat seafood, Microorganisms 7 (2019) 1–25, https://doi.org/10.3390/microorganisms7030091.
[3] A.R. Varela, O.C. Nunes, C.M. Manaia, Quinolone resistant *Aeromonas* spp. as carriers and potential tracers of acquired antibiotic resistance in hospital and municipal wastewater, Sci. Total Environ. 542 (2016) 665–671, https://doi.org/10.1016/j.scitotenv.2015.10.124.
[4] M.J. Figueras, R. Beaz-Hidalgo, *Aeromonas*, Academic Press, Norfolk, 2015, pp. 65–108.
[5] B. Lamy, A. Kodjo, F. Laurent, Prospective nationwide study of *Aeromonas* infections in France, J. Clin. Microbiol. 47 (2009) 1234–1237, https://doi.org/10.1128/JCM.00155-09.

[6] FAO, The State of World Fisheries and Aquaculture. http://www.fao.org/state-of-fisheries-aquaculture/es/, 2020 (accessed July 7, 2021).
[7] L. Santos, F. Ramos, Antimicrobial resistance in aquaculture: current knowledge and alternatives to tackle the problem, Int. J. Antimicrob. Agents 52 (2018) 135–143, https://doi.org/10.1016/j.ijantimicag.2018.03.010.
[8] A.E. Toranzo, B. Magariños, J.L. Romalde, A review of the main bacterial fish diseases in mariculture systems, Aquaculture 246 (2005) 37–61, https://doi.org/10.1016/j.aquaculture.2005.01.002.
[9] R.C. Hider, X. Kong, Chemistry and biology of siderophores, Nat. Prod. Rep. 27 (2010) 637–657, https://doi.org/10.1039/b906679a.
[10] G.E. Schulz, The structure of bacterial outer membrane proteins, Biochim. Biophys. Acta Biomembr. 1565 (2002) 308–317, https://doi.org/10.1016/S0005-2736(02)00577-1.
[11] M.J. Miller, R. Liu, Design and syntheses of new antibiotics inspired by Nature's quest for Iron in an oxidative climate, Acc. Chem. Res. 54 (2021) 1646–1661, https://doi.org/10.1021/acs.accounts.1c00004.
[12] E.L. Heil, P.D. Tamma, Cefiderocol: the Trojan horse has arrived but will Troy fall? Lancet Infect. Dis. 21 (2021) 153–155, https://doi.org/10.1016/S1473-3099(20)30828-8.
[13] J.R. Telford, J.A. Leary, L.M.G. Tunstad, B.R. Byers, K.N. Raymond, Amonabactin: characterization of a series of Siderophores from *Aeromonas hydrophila*, J. Am. Chem. Soc. 116 (1994) 4499–4500.
[14] M. Balado, A. Souto, A. Vences, V.P. Careaga, K. Valderrama, Y. Segade, J. Rodríguez, C.R. Osorio, C. Jiménez, M.L. Lemos, Two catechol Siderophores, Acinetobactin and Amonabactin, are simultaneously produced by *Aeromonas salmonicida* subsp. *salmonicida* sharing part of the biosynthetic pathway, ACS Chem. Biol. 10 (2015) 2850–2860, https://doi.org/10.1021/acschembio.5b00624.
[15] D. Rey-Varela, J. Cisneros-Sureda, M. Balado, J. Rodríguez, M.L. Lemos, C. Jiménez, The outer membrane protein FstC of *Aeromonas salmonicida* subsp. *salmonicida* acts as receptor for Amonabactin Siderophores and displays a wide ligand plasticity. Structure-activity relationships of synthetic Amonabactin analogues, ACS, Infect. Dis. 5 (2019) 1936–1951, https://doi.org/10.1021/acsinfecdis.9b00274.
[16] M. Balado, Y. Segade, D. Rey, C.R. Osorio, J. Rodríguez, M.L. Lemos, C. Jiménez, Identification of the ferric-Acinetobactin outer membrane receptor in *Aeromonas salmonicida* subsp. *salmonicida* and structure-activity relationships of synthetic Acinetobactin analogues, ACS Chem. Biol. 12 (2017) 479–493, https://doi.org/10.1021/acschembio.6b00805.
[17] R. Nudelman, O. Ardon, Y. Hadar, Y. Chen, J. Libman, A. Shanzer, Modular fluorescent-labeled siderophore analogues, J. Med. Chem. 41 (1998) 1671–1678, https://doi.org/10.1021/jm970581b.
[18] S. Noël, L. Guillon, I.J. Schalk, G.L.A. Mislin, Synthesis of fluorescent probes based on the pyochelin siderophore scaffold, Org. Lett. 13 (2011) 844–847, https://doi.org/10.1021/ol1028173.
[19] A.A. Lee, Y.C.S. Chen, E. Ekalestari, S.Y. Ho, N.S. Hsu, T.F. Kuo, T.S.A. Wang, Facile and versatile Chemoenzymatic synthesis of Enterobactin analogues and applications in bacterial detection, Angew. Chem. - Int. Ed. 55 (2016) 12338–12342, https://doi.org/10.1002/anie.201603921.
[20] Y.H. Ho, S.Y. Ho, C.C. Hsu, J.J. Shie, T.S.A. Wang, Utilizing an iron(III)-chelation masking strategy to prepare mono- and bis-functionalized aerobactin analogues for targeting pathogenic bacteria, Chem. Commun. 53 (2017) 9265–9268, https://doi.org/10.1039/c7cc05197b.
[21] P.H.C. Chen, S.Y. Ho, P.L. Chen, T.C. Hung, A.J. Liang, T.F. Kuo, H.C. Huang, T.S. A. Wang, Selective targeting of Vibrios by fluorescent Siderophore-based probes, ACS Chem. Biol. 12 (2017) 2720–2724, https://doi.org/10.1021/acschembio.7b00667.
[22] J.H. Miller, Experiments in Molecular Genetics, Cold Spring Harbor Laboratory, 1972.
[23] H. Ouchetto, M. Dias, R. Mornet, E. Lesuisse, J.M. Camadro, A new route to trihydroxamate-containing artificial siderophores and synthesis of a new fluorescent probe,, Bioorg. Med. Chem. 13 (2005) 1799–1803, https://doi.org/10.1016/j.bmc.2004.11.053.
[24] S.D. Lytton, B. Mester, J. Libman, A. Shanzer, Z. Ioav Cabantchik, Monitoring of iron(III) removal from biological sources using a fluorescent siderophore, Anal. Biochem. 205 (1992) 326–333, https://doi.org/10.1016/0003-2697(92)90443-B.
[25] J. Greenwald, F. Hoegy, M. Nader, L. Journet, G.L.A. Mislin, P.L. Graumann, I. J. Schalk, Real time fluorescent resonance energy transfer visualization of ferric pyoverdine uptake in *Pseudomonas aeruginosa*: a role for ferrous iron, J. Biol. Chem. 282 (2007) 2987–2995, https://doi.org/10.1074/jbc.M609238200.
[26] E. Bar-Ness, Y. Hadar, Y. Chen, A. Shanzer, J. Libman, Iron uptake by plants from microbial Siderophores, Plant Physiol. 99 (1992) 1329–1335, https://doi.org/10.1104/pp.99.4.1329.
[27] M.A. Walker, A high yielding synthesis of N-alkyl Maleimides using a novel modification of the Mitsunobu reaction, J. Org. Chem. 60 (1995) 5352–5355, https://doi.org/10.1021/jo00121a070.
[28] M. Delor, J. Dai, T.D. Roberts, J.R. Rogers, S.M. Hamed, J.B. Neaton, P.L. Geissler, M.B. Francis, N.S. Ginsberg, Exploiting chromophore-protein interactions through linker engineering to tune Photoinduced dynamics in a biomimetic light-harvesting platform, J. Am. Chem. Soc. 140 (2018) 6278–6287, https://doi.org/10.1021/jacs.7b13598.
[29] T. Zheng, J.L. Bullock, E.M. Nolan, Siderophore-mediated cargo delivery to the cytoplasm of *Escherichia coli* and *Pseudomonas aeruginosa*: syntheses of monofunctionalized enterobactin scaffolds and evaluation of enterobactin-cargo conjugate uptake, J. Am. Chem. Soc. 134 (2012) 18388–18400, https://doi.org/10.1021/ja3077268.
[30] J.R. Telford, K.N. Raymond, Coordination chemistry of the Amonabactins, Bis (catecholate) Siderophores from *Aeromonas hydrophila*, Inorg. Chem. 37 (1998) 4578–4583, https://doi.org/10.1021/ic980090x.
[31] C.R. Osorio, A.J. Rivas, M. Balado, J.C. Fuentes-Monteverde, J. Rodríguez, C. Jiménez, M.L. Lemos, M.K. Waldor, A transmissible plasmid-borne pathogenicity island confers piscibactin biosynthesis in the fish pathogen *Photobacterium damselae* subsp. *piscicida*, Appl. Environ. Microbiol. 81 (2015) 5867–5879, https://doi.org/10.1128/AEM.01580-15.
[32] A. Souto, M.A. Montaos, A.J. Rivas, M. Balado, C.R. Osorio, J. Rodríguez, M. L. Lemos, C. Jiménez, Structure and biosynthetic assembly of piscibactin, a siderophore from *Photobacterium damselae* subsp. *piscicida*, predicted from genome analysis, Eur. J. Org. Chem. 2012 (2012) 5693–5700, https://doi.org/10.1002/ejoc.201200818.
[33] R.G. Soengas, C. Anta, A. Espada, V. Paz, I.R. Ares, M. Balado, J. Rodríguez, M. L. Lemos, C. Jiménez, Structural characterization of vanchrobactin, a new catechol siderophore produced by the fish pathogen *Vibrio anguillarum* serotype O2, Tetrahedron Lett. 47 (2006) 7113–7116, https://doi.org/10.1016/j.tetlet.2006.07.104.
[34] A.M. Jalal, F. Jalal, M.B. Hossain, D. van der Helm, J. Sanders-Loehr, L.A. Actis, J. H. Crosa, Structure of Anguibactin, a unique plasmid-related bacterial Siderophore from the fish pathogen *Vibrio anguillarum*, J. Am. Chem. Soc. 111 (1989) 292–296.
[35] M. Balado, M.A. Lages, J.C. Fuentes-Monteverde, D. Martínez-Matamoros, J. Rodríguez, C. Jiménez, M.L. Lemos, The siderophore piscibactin is a relevant virulence factor for *Vibrio anguillarum* favored at low temperatures, Front. Microbiol. 9 (2018) 1766, https://doi.org/10.3389/fmicb.2018.01766.